Comparison of sulfide oxidizing *Sulfurimonas* strains reveals a new mode of thiosulfate formation in subsurface environments

Sven Lahme[1], Cameron M. Callbeck[2*], Lucy E. Eland[3], Anil Wipat[3], Dennis Enning[4], Ian M. Head[1] and Casey R.J. Hubert[1,5]

[1] School of Natural and Environmental Sciences, Newcastle University, Newcastle upon Tyne, United Kingdom, [2] Max Planck Institute for Marine Microbiology, Bremen, Germany, [3] School of Computing, Newcastle University, Newcastle upon Tyne, United Kingdom, [4] ExxonMobil Upstream Research Company, Spring, Texas, USA, [5] Department of Biological Sciences, University of Calgary, Calgary, Canada.

Correspondence to:
Sven Lahme, School of Natural and Environmental Sciences, Devonshire Building (3rd floor) Newcastle University, Newcastle upon Tyne, NE1 7RU, UK, Phone: +44 (0) 191 208 6011
Email: lahme.sven@gmail.com

Running title: Sulfide oxidation in Sulfurimonas spp.

* Present address: Swiss Federal Institute of Aquatic Science and Technology (Eawag), Kastanienbaum, Switzerland.

SIGNIFICANCE STATEMENT

Members of the genus *Sulfurimonas* within the class *Campylobacteria* are widespread in different environments, including in subsurface and engineered habitats such as oil fields. Understanding sulfide oxidation in these oil field bacteria has been limited by the lack of sequenced genomes, leaving inferences to be made based on the type strain, *S. denitrificans*, isolated from coastal sediment. In this study we sequenced the genome of oil field *Sulfurimonas* strain CVO to enable comparative transcriptomic analysis with *S. denitrificans* during sulfide oxidation. This uncovered key differences related to sulfide oxidation intermediates that are relevant for oil field corrosion. Comparative genomics of metagenome assembled genomes confirm that the genotype of the oil field *Sulfurimonas* strain CVO is widespread in subsurface environments, indicating widespread relevance of this alternate sulfur metabolism.

SUMMARY

Sulfur oxidizing *Sulfurimonas* spp. are widespread in sediments, hydrothermal vent fields, aquifers, and subsurface environments such as oil reservoirs where they play an important role in the sulfur cycle. We determined the genome sequence of the oil field isolate *Sulfurimonas* sp. strain CVO and compared its gene expression during nitrate-dependent sulfide oxidation to the coastal sediment isolate *Sulfurimonas denitrificans*. Formation of elemental sulfur (S^0) and high expression of sulfide quinone oxidoreductase (SQR) genes indicates that sulfide oxidation in both strains is mediated by SQR. Subsequent oxidation of S^0 was achieved by the sulfur oxidation enzyme complex (SOX). In the coastal *S. denitrificans* the genes are arranged and expressed as two clusters *soxXY$_1$Z$_1$AB* and *soxCDY$_2$Z$_2$H* and sulfate was the sole metabolic end product. By contrast the oil field strain CVO has only the *soxCDY$_2$Z$_2$H* cluster and not *soxXY$_1$Z$_1$AB*. Despite the absence of the *soxXY$_1$Z$_1$AB* cluster, strain CVO oxidized S^0 to thiosulfate and sulfate, demonstrating that *soxCDY$_2$Z$_2$H* genes alone are sufficient for S^0 oxidation in *Sulfurimonas* spp. and that thiosulfate is an additional metabolic end product. Screening of publicly available metagenomes revealed that *Sulfurimonas* spp. with only the

50 *soxCDY$_2$Z$_2$H* cluster are widespread suggesting this mechanism of thiosulfate formation is
51 environmentally significant.
52
53 **INTRODUCTION**
54 Reduced sulfur compounds such as sulfide, thiosulfate and elemental sulfur are
55 important electron donors for chemolithotrophic microorganisms in diverse habitats such as
56 marine and freshwater sediments (Howarth, 1984; Jørgensen, 1990a, 1990b; Lenk *et al.*, 2011;
57 Pjevac *et al.*, 2014), aquatic oxygen minimum zones (Jørgensen, 1982; Grote *et al.*, 2008, 2012;
58 Glaubitz *et al.*, 2010; Callbeck *et al.*, 2018), and in benthic ecosystems fueled by inorganic
59 substrates at hydrothermal vents and cold-seeps (Corre *et al.*, 2001; Takai *et al.*, 2006; Dahle
60 *et al.*, 2013; Meier *et al.*, 2017). *Sulfurimonas* spp., within the *Campylobacteria* are globally
61 distributed and abundant in these settings (Grote *et al.*, 2008; Dahle *et al.*, 2013; Pjevac *et al.*,
62 2014, 2018; Meier *et al.*, 2017). They are also versatile with respect to the oxidation of reduced
63 sulfur compounds such as sulfide, thiosulfate, and zero-valent elemental sulfur (S^0) as electron
64 donors (Han and Perner, 2015). As such, the genus *Sulfurimonas* is of considerable importance
65 in the oxidative part of the sulfur cycle. For instance, in benthic and hydrothermal settings
66 *Sulfurimonas* is often responsible for oxidizing S^0 to sulfate (Pjevac *et al.*, 2014; Meier *et al.*,
67 2017). *Sulfurimonas* spp. are also prevalent in subsurface oil reservoir and groundwater systems
68 where sulfide oxidation coupled to reduction of oxygen or nitrate has been often suggested to
69 be the key energy metabolism for these bacteria (Telang *et al.*, 1997; Shartau *et al.*, 2010;
70 Handley *et al.*, 2013; Probst *et al.*, 2018).
71 In oil fields nitrate-driven sulfur oxidation is promoted when nitrate is added externally
72 as a reservoir souring control strategy (Vigneron *et al.*, 2017). The sulfide-oxidizing and nitrate-
73 reducing ability of *Sulfurimonas* spp. and similar sulfide-oxidizing, nitrate-reducing
74 microorganisms can have major impacts on industrial processes. Stimulation of this activity has
75 been explored for mitigation of oilfield souring and corrosion control in large-scale

bioengineering strategies in oil fields (Telang *et al.*, 1997; Bødtker *et al.*, 2008; Shartau *et al.*, 2010; Gittel *et al.*, 2012; Vigneron *et al.*, 2017; Carlson and Hubert, 2019). Despite one goal of nitrate injection being corrosion control in oilfields (Hubert *et al.*, 2005; Lahme *et al.*, 2019), S^0 and other potentially corrosive sulfur compounds are often formed and excreted as intermediates during microbial sulfide oxidation (Brune, 1989; Frigaard and Dahl, 2009; Lahme *et al.*, 2019). Thus, despite their beneficial role in sulfide bioremediation, the activity of sulfide-oxidizing nitrate reducers can accelerate steel corrosion (Nemati *et al.*, 2001; Lahme *et al.*, 2019). In this regard, *Sulfurimonas* strain CVO is known to produce a variety of potentially corrosive sulfur intermediates, and can cause severe corrosion when nitrite and S^0 co-accumulate (Lahme *et al.*, 2019).

The underlying genetic basis of bacterial sulfur oxidation has been extensively studied in various sulfur oxidizing *Alpha-* and *Gammaproteobacteria*. In these organisms sulfide quinone oxidoreductases (SQR) and flavocytochrome c sulfide dehydrogenases are typically involved in catalyzing the initial oxidation of sulfide (e.g. in phototrophic green and purple sulfur bacteria; Frigaard and Dahl, 2009; Ghosh and Dam, 2009). Oxidation of sulfide by these enzymes involves formation of S^0 with polysulfide as the initial product (Griesbeck *et al.*, 2002; Berg *et al.*, 2014). These compounds are either excreted and precipitate outside the cell as biogenic S^0 particles (Schütz *et al.*, 1999; Griesbeck *et al.*, 2002) or are stored internally as sulfur globules (Frigaard and Dahl, 2009; Berg *et al.*, 2014). In addition, enzymes of the canonical reverse dissimilatory sulfate reduction (rDSR) pathway and the sulfur oxidation multi-enzyme complex (SOX) have been identified as being widespread and important mechanisms of bacterial sulfur oxidation (Kelly *et al.*, 1997; Friedrich *et al.*, 2001; Frigaard and Dahl, 2009; Ghosh and Dam, 2009).

The SOX enzyme complex in *Paracoccus pantotrophus*, a model alphaproteobacterial sulfur oxidizer, requires four enzymes for full *in vitro* activity. These are the c-type cytochromes SoxAX, the sulfur compound binding module SoxYZ, the sulfate thiol esterase

SoxB, and a sulfur dehydrogenase Sox(CD)$_2$ (Friedrich *et al.*, 2001; Rother *et al.*, 2001; Grabarczyk and Berks, 2017). During the oxidation cycle the sulfur intermediates are covalently linked to a cysteine residue in the SoxY subunit facilitated by SoxAX. Depending on the oxidation state of the terminal cysteine-bound sulfur atom SoxB will hydrolytically release sulfate either with or without Sox(CD)$_2$ performing an initial oxidation of the cysteine-persulfide to a sulfonate (Friedrich *et al.*, 2001; Grabarczyk and Berks, 2017). Therefore, in green and purple sulfur bacteria that carry only the *soxXYZAB* genes, the absence of Sox(CD)$_2$ leads to S^0 accumulation during thiosulfate oxidation (Hensen *et al.*, 2006; Frigaard and Dahl, 2009).

Currently sequenced genomes of *Sulfurimonas* spp. suggest that the oxidation of reduced sulfur compounds likely involves the SOX system as well as different types of SQR enzymes (Sievert *et al.*, 2008; Sikorski *et al.*, 2010; Grote *et al.*, 2012; Cai *et al.*, 2014; Han and Perner, 2015). Unlike many alphaproteobacterial sulfur oxidizers (e.g. *P. pantotrophus*, *Rhodopseudomonas palustris*, *Rhodovulum sulfidophilum* and *Starkeya novella*), which carry the *soxABCDXYZ* genes in a single gene cluster (Ghosh and Dam, 2009), *Sulfurimonas* spp. contain two separate *sox* clusters, i.e., *soxXY$_1$Z$_1$AB* and *soxCDY$_2$Z$_2$* (Sievert *et al.*, 2008; Sikorski *et al.*, 2010; Grote *et al.*, 2012; Cai *et al.*, 2014). Both clusters contain homologs of *soxYZ*, which show a high level of divergence and are proposed to be involved in oxidation of different sulfur compounds (Meier *et al.*, 2017; Pjevac *et al.*, 2018). The organization of separate *sox* gene clusters in *Sulfurimonas* spp. may indicate a loss of co-dependency of the individual genes for oxidation of certain sulfur compounds; indeed, both gene clusters appear to be differentially regulated in *Sulfurimonas denitrificans* DSM 1251 when growing on zero-valent cyclooctasulfur (S_8) compared to thiosulfate (Götz *et al.*, 2019).

To advance our understanding of sulfur cycling by sulfide-oxidizing, nitrate-reducing microorganisms and *Sulfurimonas* spp. in particular we sequenced the genome of the oil-field isolate *Sulfurimonas* sp. strain CVO and studied its gene expression during the oxidation of

sulfide and biogenic elemental S^0. We compared the genome and transcriptome of strain CVO with the closely related *S. denitrificans* DSM 1251 under the same growth conditions to detect genotypic and metabolic differences. Our findings confirmed a newly proposed role of the *sox* gene products in S^0 oxidation (Götz *et al.*, 2019) and reveal a new and likely widespread mechanism for thiosulfate formation. In addition, we provide evidence for different modes by which *Sulfurimonas* spp. form biofilms that help better explain their competitiveness in natural and industrial systems.

RESULTS

Formation of relevant intermediates during sulfide and elemental S^0 oxidation

When supplied with sulfide and excess nitrate both *Sulfurimonas* sp. strain CVO and *Sulfurimonas denitrificans* immediately oxidized all sulfide to near equal amounts of S^0 (Fig. 1). This was accompanied by the development of a yellow coloration in the medium, indicating polysulfide formation (Steudel, 1996), as well as a grey precipitate indicating the formation of elemental S^0. After sulfide had been consumed, the yellow color disappeared and the precipitated S^0 was further oxidized by both strains. Whereas, *S. denitrificans* completely oxidized all S^0 to 2.2 mM sulfate (Fig. 1B), strain CVO accumulated 1.1 mM thiosulfate and 0.9 mM sulfate (Fig. 1A). Sulfite appeared transiently during the growth of strain CVO, reaching up to 0.6 mM before being consumed. In strain CVO, thiosulfate, once formed, remained constant, suggesting it is a metabolic end-product of S^0 oxidation (Fig. 1A). When supplied only with 10 mM biogenic S^0 and nitrate, strain CVO and *S. denitrificans* oxidized S^0 at rates of 7.9 and 6.1 $\mu mol \cdot h^{-1}$, respectively (Fig. S1), about eight (59.1 $\mu mol \cdot h^{-1}$) and four times (21.7 $\mu mol \cdot h^{-1}$) lower than the oxidation of intermediate S^0 in sulfide-grown cultures (Fig. 1). Interestingly, strain CVO grown on S^0 oxidized it almost completely to sulfate, forming <0.2 mM of both sulfite and thiosulfate (Fig. S1), whereas sulfite and thiosulfate were absent in cultures of *S. denitrificans* grown on S^0.

Oxidation of sulfide and S^0 was coupled to the reduction of nitrate by both organisms (Fig. 1, Fig. S1). Both of these *Sulfurimonas* spp. reduce nitrate to dinitrogen gas via denitrification (Timmer-Ten Hoor, 1975; Gevertz *et al.*, 2000; Sievert *et al.*, 2008). Strain CVO reduced nitrate and accumulated up to 2.6 mM nitrite, accounting for 38% of the total nitrate consumed (Fig. 1A). *S. denitrificans* on the other hand did not accumulate any detectable nitrite intermediate (Fig. 1B). While growth rates were not explicitly determined in this study, doubling times have been reported as 1.3 h for strain CVO growing with sulfide and nitrate (Gevertz *et al.*, 2000) and 8 h and 11 h for *S. denitrificans* growing with either thiosulfate or S_8 (Götz *et al.*, 2018). Growth was tracked in the present study based on measurement of total RNA over the time course of the experiments (Figure S2).

General comparison of *Sulfurimonas* genomes and transcriptomes

Whole genome sequencing of strain CVO revealed a single circular 1.92 Mbp chromosome containing 1957 genes of which 1885 were protein coding (Table 1). While this represents the smallest genome of the genus *Sulfurimonas*, the tRNA coding genes and rRNA operons are similar to the other sequenced genomes within this genus (Table 1). A broad comparison of the genomes of strain CVO and *S. denitrificans* via clusters of orthologous groups of proteins (COG) classifications revealed similar gene abundances for most COG categories (Fig. 2). COG analysis also showed that strain CVO contains noticeably fewer genes involved in cell motility and signal transduction compared to *S. denitrificans*.

To examine changes in gene expression specifically associated with the oxidation of sulfide and S^0, we examined the transcriptomes of strain CVO and *S. denitrificans* using cells harvested at two different times: during active sulfide oxidation, and during active S^0 oxidation (Fig. 1). In addition, for *S. denitrificans* the transcriptome of cells grown on thiosulfate was obtained for further comparison (Fig. S1A). Transcriptomes were analyzed from triplicate cultures, and always showed a similar distribution of mapped reads across the genome (Fig. S3). Both organisms also showed similar expression values for COG categories measured as

fragments per kilobase and million reads (FPKM; Fig. S4). A total of 1832 and 1839 gene transcripts were detected in the transcriptomes of strain CVO during oxidation of sulfide and S^0, respectively, corresponding to 97–98% of all protein coding genes (Table 2). Among those transcripts 588 significantly increased (≥1.5-fold) and 528 significantly decreased (≤1.5-fold) during S^0 oxidation, relative to the sulfide oxidation phase. Similarly, for *S. denitrificans* between 1949 and 2036 transcripts were detected during oxidation of sulfide and S^0, respectively (92–97% of protein coding genes), with 612 and 534 showing significantly increased and decreased abundances, respectively, during oxidation of S^0 (Table 2).

Different *sox* clusters and gene expression between two strains of *Sulfurimonas*

The genome of strain CVO contains several putative homologs of sulfide quinone oxidoreductase (SQR) enzymes, which based on amino acid sequence alignments cluster with type II (SqrB), type IV (SqrD) and type VI (SqrF) enzymes (Fig. S5). *S. denitrificans* contains SqrB and SqrD enzymes as well but lacks SqrF and instead harbours a type III (SqrC) enzyme. The transcripts from all *sqr* genes were detected in strain CVO and *S. denitrificans* (Fig. 3). However, both strains showed significantly higher expression of *sqrB* and *sqrD* in the S^0 oxidation phase despite the depletion of sulfide at the point of RNA extraction (Fig. 1). *S. denitrificans* also expressed *sqrB* and *sqrD* during the oxidation of thiosulfate (Table S1). In contrast, transcript abundances of *sqrF* associated to strain CVO, and of *sqrC* associated to *S. denitrificans*, were expressed at much lower levels during both sulfide and S^0 oxidation.

Unlike other *Sulfurimonas* genomes that possess two separate *sox* gene clusters (Fig. 4B), strain CVO lacks a *soxXY$_1$Z$_1$AB* gene cluster and contains only the *soxCDY$_2$Z$_2$* gene cluster (Fig. 4A). Cross-mapping of DNA and RNA sequence reads obtained from CVO cultures against the genome of *S. denitrificans* confirmed the absence of a *soxXY$_1$Z$_1$AB* gene cluster in strain CVO (Fig. S6). Genbank searches for *Sulfurimonas* metagenomes from both marine and terrestrial system revealed that among 35 metagenome-assembled genomes (MAGs), only 20 contained both gene clusters, while 15 have the strain CVO genotype of only the *soxCDY$_2$Z$_2$*

206 gene cluster (Fig. 4C). No *Sulfurimonas* MAGs or pure culture genomes contain only the
207 *soxXY$_1$Z$_1$AB* gene cluster. This provides strong evidence that the genotype observed in strain
208 CVO might occur in other *Sulfurimonas* spp. particularly those in the terrestrial subsurface (Fig.
209 4C).

210 In all *Sulfurimonas* genomes the *soxCDY$_2$Z$_2$* genes are located adjacent to a gene
211 annotated as putative metallo hydrolase (protein superfamily SSF56281) that bears some
212 similarity to the *soxH* gene of *P. pantotrophus* (23% protein sequence identity), that was
213 annotated as a thiol hydrolase (Friedrich *et al.*, 2001; Götz *et al.*, 2019). While *S. denitrificans*
214 showed high expression of the *soxCDY$_2$Z$_2$H* cluster during oxidation of sulfide and S^0 (Fig.
215 3B), strain CVO showed enhanced expression only during S^0 utilization phase (up to a 49-fold
216 increase relative to during sulfide oxidation; Fig. 3A). A similar response was seen for the
217 *soxXY$_1$Z$_1$AB* cluster in *S. denitrificans* (Fig. 3B). *S. denitrificans* expressed both *sox* clusters
218 during thiosulfate oxidation (Table S1), in agreement with the involvement of this gene cluster
219 in the oxidation of thiosulfate (Friedrich *et al.*, 2001). Two sets of genes for putative polysulfide
220 reductase-like molybdoenzymes (*psrA$_1$B$_1$C$_1$* and *psrA$_2$B$_2$C$_2$*) were found in the CVO genome,
221 and at least one set is present in all other *Sulfurimonas* genomes (Fig. 4C). Both strain CVO
222 and *S. denitrificans* expressed all *psr* genes during either sulfide or S^0 oxidation (Fig. 3) likely
223 due to the formation of polysulfide in both cultures.

224 **Surface adhesion and motility gene expression differ in two *Sulfurimonas* strains**

225 Oxidation of insoluble solid S^0 is frequently suggested to involve attachment of cells to
226 S^0 particles and expression of outer membrane proteins (OMP; Buonfiglio *et al.*, 1993; Ramírez
227 *et al.*, 2004; Mangold *et al.*, 2011; Chen *et al.*, 2012). In agreement with this requirement both
228 *Sulfurimonas* spp. tested here formed dense biofilms on elemental S^0 particles (Fig. S7). The
229 highest expression level in the transcriptome of strain CVO during S^0 oxidation was observed
230 for a gene annotated as hypothetical protein (CVO_00715; Fig. 5A) with amino acids 3 to 187
231 having high similarity with the OprD-like porin superfamily (cl21675) and the major outer

membrane proteins of *Campylobacter* (pfam05538). Modeling of structural topology (BOCTOPUS2, PRED-TMBB2 and Phyre2) revealed several potential transmembrane domains predicted to form a β-barrel-like structure, indicative of a role as an outer membrane protein (Tommassen, 2010). The most similar gene in the genome of *S. denitrificans*, Suden_1917 (57% protein sequence identity), was also the most highly expressed gene in the S^0 oxidation phase (Fig. 5B) and has similar predicted protein domain structures (Götz *et al.*, 2019). Both strains showed a significant increase in expression of their OprD-like genes during S^0 oxidation relative to the sulfide oxidation phase. Furthermore, each strain showed significant changes in the expression of additional OprD- or OmpA-type outer membrane porin genes, but those were expressed at much lower levels overall (Fig. 5, Table S1).

During the S^0 oxidation phase strain CVO also displayed significantly higher expression (1.5- to 3.5-fold *vs.* sulfide oxidation phase) of several genes for a type IV pilus machine (Fig. 5A, Table S1). Type IV pili are frequently involved in surface adhesion and gliding motility (Craig *et al.*, 2019). A protein sequence comparison against the curated UniprotKB protein database Swiss-prot revealed that the genes CVO_03020, CVO_03025, CVO_03705 and CVO_07430 share between 30–50% amino acid sequence identity with proteins of the type IV pilus machine from *Pseudomonas aeruginosa* DSM 22644 (Table S1). Strain CVO also expressed several potential pilin genes (Fig. 5A) that contain the pilin-specific N-terminal cleavage site (TIGR02532). While most of the pilin genes showed similar expression behaviour to the type IV biogenesis and twitching motility genes, the gene CVO_07920 showed remarkably high expression during both sulfide and S^0 oxidation (Fig. 5A). In stark contrast, *S. denitrificans* showed nearly no expression of most of its homologs of these genes (Fig. 5B).

During the S^0 oxidation phase strain CVO also exhibited an increase in gene expression of 2.1 up to 11.3-fold of genes related to a type I secretion systems (CVO_05415-05425), a protein containing a cadherin tandem repeat domain (PF00028; CVO_05435), as well as a 1083 amino acid long complex protein (CVO_05445) related to repeats in toxin (RTX) proteins

(COG2931). The latter gene contains several protein domains typically found in RTX-related proteins, including cadherin-like (PF17803), *Vibrio-Colwellia-Bradyrhizobium-Shewanella* (VCBS) repeat (TIGR01965), hemolysin-type calcium binding (PF00353) and serralysin-like metalloprotease (PF08548) domains, consistent with type I mediated secretion and suggestive of involvement in biofilm cell adhesion (Satchell, 2011). Interestingly, the genome of *S. denitrificans* lacks a homolog to CVO_05445, but contains an orthologous RTX-related gene, Suden_1200, which has similar domains (PF00353 and PF08548) but lacks the VCBS repeat. Like the CVO genes, Suden_1200 in *S. denitrificans* also showed increased expression (3.9-fold) during S^0 oxidation compared to sulfide oxidation (Fig. 5B).

Strain CVO has been described previously as non- or only weakly motile (Gevertz *et al.*, 2000). In agreement with previous work, our genome analysis of strain CVO reveals the absence of flagellar genes required for motility, and contains only putative homologs of the flagellar hook-basal body protein (*fliF*, CVO_07390) and the flagellar motor switch proteins *fliG* (CVO_07385) and *fliNM* (CVO_06450, CVO_06455) that are typically located on the cytoplasmic site of cell membranes (Minamino and Imada, 2015). Despite the general absence of motility genes, CVO did express *fli* genes, albeit, at a low level (Fig. 6A). By contrast, *S. denitrificans* possesses all genes required to form a functional flagellum (Sievert *et al.*, 2008) and these were expressed during the oxidation of sulfide and S^0 (Fig. 6B). However, significantly higher expression of *S. denitrificans* flagellar genes was observed in S^0 oxidizing cells compared to sulfide or thiosulfate oxidizing cells (Fig. 6B, Table S1), similar to a recent report for S_8 oxidizing *S. denitrificans* cells (Götz *et al.*, 2019).

DISCUSSION

Sulfide oxidation in *Sulfurimonas* spp. involves constitutively expressed SQR genes

Previous studies generally ascribe the accumulation of biogenic elemental S^0 to the microbial oxidation of sulfide under both aerobic and anaerobic conditions (Brune, 1989;

Frigaard and Dahl, 2009; Ghosh and Dam, 2009). Cultivation of *Sulfurimonas* sp. strain CVO and *Sulfurimonas denitrificans* with sulfide and nitrate resulted in the accumulation of S^0 as a metabolic intermediate during anaerobic sulfide oxidation (Fig. 1). In both *Sulfurimonas* sp. strain CVO and *Sulfurimonas denitrificans,* high expression of several sulfide quinone oxidoreductase genes as well as formation of intermediate S^0 (Fig. 1 and 3) strongly support the interpretation that SQR-mediated sulfide oxidation is occurring in both species (Griesbeck *et al.*, 2002). In addition, formation of intermediate S^0 would not be expected if sulfide is oxidized via the SOX enzyme system, as the sulfur substrate would remain bound to the SoxYZ enzyme (Friedrich *et al.*, 2001; Grabarczyk and Berks, 2017). Although S^0 formation has been observed in cultures of strain CVO before (Gevertz *et al.*, 2000; Lahme *et al.*, 2019), to our knowledge this has not been shown for other *Sulfurimonas* spp. Our results therefore support the general view that formation of S^0 from sulfide oxidation is a common phenotype of this genus (Han and Perner, 2015).

Our results also reveal that bulk sulfide oxidization in *Sulfurimonas* is likely achieved by the type II SqrB and type IV SqrD enzymes, which are present in all isolated *Sulfurimonas* spp. (Fig. S5). SqrB and SqrD are expressed at high levels in both strains examined in this study (Fig. 3), consistent with SQR of *Campylobacteria* often being strongly expressed in sulfidic habitats (Dahle *et al.*, 2013; Handley *et al.*, 2013; Jewell *et al.*, 2016; Pjevac *et al.*, 2018). Although *in vitro* activity of all three SQR from *S. denitrificans* was recently shown (Han and Perner, 2016), the comparably low expression of *sqrC* in *S. denitrificans* and *sqrF* in strain CVO point towards marginal involvement of these genes in sulfide oxidation under these experimental conditions. Higher expression of *sqrB* and *sqrD* during S^0 oxidation (and during thiosulfate oxidation in *S. denitrificans*) also suggests that they are constitutively expressed, possibly to enable a rapid response to sulfide availability. Both genes were also expressed by *S. denitrificans* during growth on H_2 (Han and Perner, 2016), and the purple sulfur bacterium

309 *Allochromatium vinosum* expresses *sqr* during oxidation of various sulfur substrates, not only
310 sulfide (Weissgerber *et al.*, 2013).

311 **Oxidation of S^0 in *Sulfurimonas* spp. requires only one of two *sox* clusters**

312 Strain CVO is the first isolated *Sulfurimonas* strain with a sequenced genome that lacks
313 the *soxXY$_1$Z$_1$AB* gene cluster (Fig. 4A). Despite these missing *sox* genes, strain CVO still
314 showed clear S^0 oxidation activity (Fig. 1A and S1B) coupled with high expression of its
315 *soxCDY$_2$Z$_2$* genes (Fig. 3A). Involvement of the *sox* gene products in biological S^0 oxidation
316 was recently proposed for *S. denitrificans*, with proteomic analysis of S_8 grown cells revealing
317 only protein products of the *soxCDY$_2$Z$_2$H* cluster whereas *soxXY$_1$Z$_1$AB* protein products were
318 below detection (Götz *et al.*, 2019). Our results with strain CVO clearly show that products of
319 the *soxCDY$_2$Z$_2$H* gene cluster are sufficient for biological S^0 oxidation in *Sulfurimonas* spp.
320 These results support the hypothesis that *sox* gene clusters in *Sulfurimonas* spp. evolved to
321 support energy metabolism with different sulfur compounds, either cooperating in the oxidation
322 of thiosulfate or operating independently during the oxidation of S^0 (Meier *et al.*, 2017; Götz *et*
323 *al.*, 2019).

324 The absence of the *soxXY$_1$Z$_1$AB* cluster in strain CVO is consistent with its inability to
325 utilize thiosulfate (Gevertz *et al.*, 2000) and explains why thiosulfate, once formed, is not
326 further oxidized (Fig. 1A). The lack of the *soxB* gene in strain CVO raises the question of how
327 the sulfonate group is released from the enzyme. Götz and colleagues (2019) speculated that
328 the product of the *soxH*-like gene, a putative metallo hydrolase, releases sulfate from SoxY
329 (Fig. 4). The genetic co-localization and co-expression of this *soxH*-like gene with the
330 *soxCDY$_2$Z$_2$* genes in both strain CVO and *S. denitrificans* suggest involvement of SoxH in S^0
331 oxidation is plausible. Further genetic and biochemical studies are needed to verify the exact
332 role of SoxH in bacterial S^0 oxidation.

333 **Missing *sox* cluster result in formation of additional sulfur compounds**

Aerobic and phototrophic S^0 oxidizing bacteria and archaea have shown sulfur oxidation phenotypes similar to that of CVO, yielding sulfite, thiosulfate and sulfate as intermediates or end products (Brune, 1989; Kletzin, 1989; Rohwerder and Sand, 2003; Frigaard and Dahl, 2009; Xia *et al.*, 2017). However, in these microorganisms, oxygen-dependent enzyme systems (e.g. sulfur oxygenases or persulfide dioxygenase), or enzymes of the reverse dissimilatory sulfate reduction (rDSR) pathway, are instead responsible for the oxidation of S^0 and the production of sulfite. Strain CVO possesses neither sulfur compound-specific (di)oxygenases nor enzymes of the rDSR pathway, suggesting that the accumulation of sulfite and thiosulfate intermediates is linked to the lack of *soxXY$_1$Z$_1$AB*, since sulfite and thiosulfate were not detected in cultures of *S. denitrificans* that carries both gene clusters (Fig. 1 and 4).

The current model for the Sox(CD)$_2$-mediated oxidation of the SoxY-Cys persulfide anion involves iterative hydroxylation steps to yield SoxY-Cys-S-sulfinate as an intermediate and SoxY-Cys-S-sulfonate as final oxidation product (Zander *et al.*, 2011). We therefore posit that the sulfite detected in CVO cultures is a by-product of incomplete oxidation of S^0 as a result of the truncated SOX enzyme system, possibly due to premature release of the SoxY-bound sulfur substrate at the level of a SoxY-Cys-S-sulfinate and involving SoxH (Fig. S8). In *S. denitrificans* the low expression of the *soxXY$_1$Z$_1$AB* cluster (Fig. 3B) could still produce sufficient quantities of SoxAX and SoxB enzymes to prevent accumulation of sulfite and thiosulfate (Fig. S8). Strain CVO lacks both SoxAX and SoxB, allowing produced sulfite to rapidly react with S^0 or polysulfides to form thiosulfate as observed during aerobic sulfide and S^0 oxidation (Kletzin, 1989; Rohwerder and Sand, 2003; Xia *et al.*, 2017). Interestingly, accumulation of sulfite and thiosulfate was less pronounced when strain CVO was grown on S^0 that had been harvested from other cultures and added to the medium (Fig. S1B). This suggests that during sulfide oxidation reactive sulfur species such as polysulfides might accelerate abiotic reactions that lead to sulfite and thiosulfate accumulation.

Thiosulfate is an important intermediate in the global sulfur cycle (Jørgensen, 1990a, 1990b). Its formation due to a truncated version of the SOX enzyme system in strain CVO and other *Sulfurimonas* spp. (Fig. 4C) represents a novel mechanism for thiosulfate accumulation in sediments and other habitats that harbor organisms with a similar genetic arrangement. The rate by which thiosulfate is formed, however, might also depend on individual environmental conditions such as presence of reactive sulfur species. Several genomes of *Sulfurimonas*- and also *Sulfurovum*-like organisms from the terrestrial subsurface reveal the CVO genotype of only the *soxCDY$_2$Z$_2$H* genes and not the *soxXY$_1$Z$_1$AB* genes (Handley *et al.*, 2013; Anantharaman *et al.*, 2016; Jewell *et al.*, 2016). This suggests that organisms with a similar sulfur oxidation phenotype to strain CVO are found in subsurface environments. While strain CVO is the first *Sulfurimonas* sp. from an oil reservoir with a complete genome sequence, these and other *Campylobacteria* are prominent in oil field settings (Hubert *et al.*, 2012) where S intermediates are postulated to influence microbe-microbe interactions (Telang *et al.*, 1999) and impact corrosion of metal infrastructure (Lahme *et al.*, 2019).

Sulfurimonas spp. adhere to S^0 particles by different mechanisms

Low water solubility and steric limitation during the oxidation of solid S^0 require bacterial cells to attach to S^0 surfaces to facilitate its degradation (Schaeffer *et al.*, 1963; Ohmura *et al.*, 1996; Rohwerder and Sand, 2003; Mangold *et al.*, 2011; Pjevac *et al.*, 2014). Flagella play an important role in initial biofilm development in various bacteria and archaea (O'Toole and Kolter, 1998; Pratt and Kolter, 1998; Ottemann and Lowenthal, 2002; Kalmokoff *et al.*, 2006; Jarrell *et al.*, 2011; Svensson *et al.*, 2014) and flagellar proteins have been suggested to mediate attachment to sulfur particles in pure cultures of *Acidithiobacillus ferrooxidans*, *Ac. caldus* and *S. denitrificans* grown on S^0 (Ohmura et al. 1996; Mangold et al. 2011; Götz et al. 2019). In the case of *Ac. ferrooxidans* deflagellated cells also attached to S^0 particles, implying alternate mechanisms that contribute to surface adhesion (Ohmura *et al.*, 1996). Strain CVO lacks genes for surface-associated flagellar proteins (Fig. 6) and exhibited

385 greater S^0 oxidation ability than *S. denitrificans* in the present study (Fig. 1 and Fig. S1),
386 implying that flagella are not essential for S^0 oxidation in *Sulfurimonas* spp.

387 Strong expression of pilin-like and twitching motility proteins by strain CVO suggest
388 that type IV pili might be involved in biofilm development during S^0 oxidation, potentially
389 compensating for the absence of flagella. Type IV pilin-like proteins are often involved in
390 mediating adhesion to abiotic surfaces and contribute to biofilm development in various
391 bacteria and archaea (Barken *et al.*, 2008; Jarrell *et al.*, 2011; Richter *et al.*, 2012). Expression
392 of twitching motility proteins might contribute to gliding along surfaces and also indicate how
393 the cells shift their physiology towards a biofilm lifestyle. Strain CVO also increased expression
394 of a type I secretion system and a gene for an RTX-related protein, both gene products
395 potentially involved in adhesion. RTX protein VCBS-repeat and cadherin-like domains have
396 been shown to mediate binding to abiotic surfaces (Hinsa *et al.*, 2003; Nishikawa *et al.*, 2016).
397 The domain structure of the RTX-type protein in strain CVO and its elevated gene expression
398 during S^0 oxidation suggest it could play a role in surface attachment. Cadherin-like domains
399 could additionally support biofilm stability by mediating cell-cell contact or interaction with
400 exopolysaccharides in a biofilm matrix (Fraiberg *et al.*, 2012; Vozza *et al.*, 2016).

401 Overall *S. denitrificans* and strain CVO likely adhere to S^0 particles via different
402 mechanisms. Whereas flagellum-mediated adhesion might be pivotal for *S. denitrificans* (Götz
403 *et al.*, 2019), strain CVO appears to employ alternative mechanisms. Like other Gram-negative
404 biofilm forming bacteria, *Sulfurimonas* spp. likely utilize more than just one mechanism for
405 surface attachment (Pratt and Kolter, 1998; Barken *et al.*, 2008). Diverse surface attachment
406 mechanisms and their ability to utilize a variety of electron donors and acceptors (Han and
407 Perner, 2015) could explain the persistence of *Sulfurimonas* spp. in various ecosystems and
408 their prevalence following natural or anthropogenic perturbations in subsurface and industrial
409 environments (Telang *et al.*, 1997; Bødtker *et al.*, 2008; Handley *et al.*, 2013; Jewell *et al.*,
410 2016; Wu *et al.*, 2017; Probst *et al.*, 2018). In oil field settings, adhesion mechanisms employed

411 by *Sulfurimonas* strain CVO and other *Campylobacteria* may also allow for biofilm formation
412 on steel surfaces and contribute to pitting corrosion that has been observed in association with
413 these bacteria (Nemati *et al*., 2001; Hubert *et al*., 2005; Lahme *et al*. 2019).

414 The frequently observed high expression of specific outer membrane proteins (OMP) in
415 cells oxidizing solid sulfur substrates suggests an important involvement in utilizing those
416 substrates (Buonfiglio *et al.*, 1993; Ramírez *et al.*, 2004; Mangold *et al.*, 2011; Chen *et al.*,
417 2012). Recently, an OMP (Suden_1917) from *S. denitrificans* DSM 1251 was implicated in the
418 utilization of solid S_8 due to its abundance in S_8 oxidizing cells compared to cells oxidizing
419 thiosulfate (Götz *et al.*, 2019). Our observation from *S. denitrificans* corroborate this, as does
420 our finding that the gene with the highest expression during S^0 oxidation in strain CVO encode
421 a homolog of this cell surface protein. It remains an open question whether this protein is
422 directly involved in degradation of S^0, or facilitates the transport of S^0 into the cell. Although
423 some sulfur oxidizing bacteria utilize S^0 substrates via glutathione persulfide intermediates
424 (Rohwerder and Sand, 2003; Xin *et al.*, 2016), this system is absent in both *Sulfurimonas* strains
425 because they lack key enzymes such as glutathione synthetase (Sievert *et al.*, 2008).
426
427 **CONCLUSION**

428 *Sulfurimonas* spp. are key-players during nitrate-mediated souring control in moderate
429 temperature oil reservoirs (Telang *et al.*, 1997; Bødtker *et al.*, 2008) such as the 30°C oil field
430 from which strain CVO was isolated (Gevertz *et al.*, 2000). Accordingly, *Sulfurimonas* spp. are
431 of interest in relation to their potential to mitigate negative aspects of oil field sulfur cycling
432 (Carlson and Hubert, 2019) even though their activity has also been shown to cause severe
433 corrosion (Lahme *et al.*, 2019). The work presented here advances our understanding of genetic
434 mechanisms for accumulation of corrosive sulfur compounds (e.g. S^0 or thiosulfate) and the
435 rapid formation of *Sulfurimonas* biofilms. Comparing the genome, transcriptome and sulfur
436 biochemistry of two closely related *Sulfurimonas* spp. revealed genetic and physiological

differences that highlight alternative mechanisms of sulfur oxidation in natural and engineered systems. SQR mediated oxidation of sulfide and subsequent S^0 production is a common metabolic trait among *Sulfurimonas* spp. Subsequent oxidation of this S^0 intermediate requires products of only one of the two known *sox* gene clusters, namely *soxCDY*$_2$*Z*$_2$*H*, in *Sulfurimonas* spp. and likely in other *Campylobacteria.* Our results also reveal a novel mode of thiosulfate formation that does not seem to be exclusive to strain CVO, but is widespread among other *Sulfurimonas* spp. This has implications for sulfur cycling in sedimentary and other subsurface systems related to other sulfur metabolisms such as thiosulfate disproportionation (Finster *et al.*, 1998). Comparative transcriptomics also showed how *Sulfurimonas* spp. direct their metabolism towards biofilm development as solid S^0 accumulates, but that different mechanisms for surface attachment exist in different organisms. The presence of type-IV pili potentially explains how *Sulfurimonas* spp. are able to rapidly form biofilms and withstand changing environmental conditions in various habitats (Telang *et al.*, 1997; Bødtker *et al.*, 2008; Wu *et al.*, 2017; Probst *et al.*, 2018).

EXPERIMENTAL PROCEDURES

Strains and growth conditions

Sulfurimonas sp. strain CVO (NRRL B-21472) was obtained from the Agricultural Research Service Culture Collection Northern Regional Research Laboratory (ARS NRRL, US). *Sulfurimonas denitrificans* DSM 1251 was obtained from the German Collection of Microorganisms and Cell Cultures (DSMZ). Strain purity was verified by microscopy and sequencing of the 16S rRNA gene.

Strains were routinely cultured under anaerobic conditions in modified Coleville synthetic brine medium (CSB-A) at 20 °C as recently described (Hubert *et al.*, 2003; Lahme *et al.*, 2019). For cultivation of *S. denitrificans* addition of NaCl was omitted as it inhibited growth. For cultures initiated on S^0 as the starting substrate, biogenic S^0 from strain CVO or *S.*

463 *denitrificans* was harvested and used as described elsewhere (Lahme *et al.*, 2019). Sodium
464 nitrate (2 M), and sodium sulfide, biogenic S^0 or sodium thiosulfate (both 1 M) were added
465 from anoxic stock solutions by means of N_2-flushed syringes (see supplementary methods for
466 further details).

467 Gene expression during sulfur compound oxidation coupled with nitrate reduction was
468 assessed in triplicate cultures of strains CVO (4 mM sulfide, 10 mM nitrate) or *S. denitrificans*
469 (2 mM sulfide or 5 mM thiosulfate, and 10 mM nitrate), respectively. For individual
470 experiments 5% (v/v) of three-day old cultures adapted to the respective substrates for five
471 consecutive transfers served as inocula.

472 **Chemical analysis**

473 Samples were taken from cultures with N_2-flushed syringes and either directly analyzed,
474 frozen at –20° C or treated according to specific methodological requirements before freezing
475 as described recently by Lahme et al. (2019). Dissolved sulfide concentrations were directly
476 determined after filtration (0.2 µm, cellulose-acetate) using the spectrophotometric $CuSO_4$
477 method (Cord-Ruwisch, 1985). Concentrations of nitrate, nitrite and sulfate were determined
478 by ion chromatography, and biogenic S^0 was measured by liquid chromatography after
479 extraction with chloroform as described elsewhere (Lahme *et al.*, 2019). Thiosulfate and sulfite
480 were quantified by liquid chromatography after derivatization with monobromobimane as
481 described elsewhere (Callbeck *et al.*, 2018; Lahme *et al.*, 2019). While other sulfur
482 intermediates can potentially form due to interactions between different compounds, no other
483 sulfur compounds were quantified.

484 **Nucleic acid sampling and extraction**

485 Cells of strain CVO were harvested from 200 ml freshly grown culture grown with 4
486 mM sulfide and 10 mM nitrate by centrifugation (10 min at 5,000 g and 4° C) and washed in
487 Tris-EDTA buffer (TE; 100 mM Tris, 1 mM EDTA, pH 8.0). Cells were subsequently lysed
488 using consecutive lysozyme, proteinase K and sodium dodecyl sulfate treatments, RNA

digested by RNase A and DNA extracted by phenol chloroform isoamylalcohol. After ethanol precipitation the DNA pellet was air dried, resuspended in TE buffer (see above) and then frozen in aliquots at –20° C (see supplementary methods for further details).

For RNA extraction, cells from triplicate cultures for each strain were harvested during active oxidation of sulfide or biogenic elemental S^0, as well as thiosulfate in case of *S. denitrificans* (see arrows in Fig. 1 and Fig. S1). Samples were removed using N_2-flushed syringes and stabilized using RNAprotect® Bacterial Reagent (Qiagen, UK) and the cell pellet frozen at –80° C prior to extraction. RNA was extracted using the Isolate II RNA mini kit (Bioline, UK) including two DNase I treatments. After cleaning and concentrating using the Zymo Research RNA Clean and Concentrator-5 (Cambridge Biosciences Ltd., UK), the RNA was aliquoted and stored at –80° C. Removal of DNA was verified by PCR and RNA integrity controlled on an Agilent 2100 Bioanalyzer (Agilent Technologies, UK) with the RNA 6000 Nano assay (see supplementary methods for further details).

DNA and RNA purity were assessed with a NanoDrop® ND-1000 spectrophotometer (Thermo Fisher Scientific, UK) and concentration was additionally confirmed using an Invitrogen Qubit® 3.0 Fluorometer (Thermo Fisher Scientific, UK).

DNA sequencing, assembly and annotation

DNA from strain CVO was sequenced at the Centre for Genomic Research (CGR) at the (Liverpool University, UK) on a Pacific Bioscience RSII platform using a 10kb library preparation protocol and P6-C4 chemistry on a Single Molecule Real-Time (SMRT®) cell. Additional paired-end sequencing (2x 300 bp) was performed at the Centre for Bacterial Cell Biology (Newcastle University, UK) on an Illumina MiSeq platform using the Miseq v3 reagent kit and Nextera XT kit (Illumina, UK) for library preparation.

After quality and adapter trimming of sequencing reads, *de novo* genomes were assembled with the SPAdes Genome Assembler (v 3.6.2) using the hybrid assembly function (Bankevich *et al.*, 2012) and the resulted in single high coverage scaffold, which was manually

515 closed by merging overlapping ends in Artemis (Rutherford *et al.*, 2000). Structural and
516 functional annotation was performed using the National Center for Biotechnology Information
517 (NCBI) prokaryotic annotation pipeline (Tatusova *et al.*, 2016; Haft *et al.*, 2018). Functional
518 predictions of genes referred to in this study were inspected by comparing the automatic
519 annotation to InterPro scans (Mitchell *et al.*, 2019) and BLASTP comparison against the NCBI
520 non-redundant protein sequence (Camacho *et al.*, 2009) or the UniProtKB/Swiss-Prot protein
521 sequence database (Boutet *et al.*, 2007).

522 The sequencing reads used for *de novo* genome reconstruction have been deposited at
523 the NCBI Sequence Read Archive (SRA) under the accession number PRJNA482764.The
524 annotated genome from strain CVO has been deposited at GenBank under accession number
525 CP033720.

526 **RNA sequencing and differential gene expression analysis**

527 For RNA sequencing libraries, rRNA was first removed using the Ribo-Zero rRNA
528 Removal Kit for bacteria (Illumina, UK). Subsequently, RNA sequencing libraries were
529 prepared using the ScripSeq v2 kit according to manufacturer's instructions. Paired-end
530 sequencing (2x 125bp) of multiplexed libraries was performed at the CGR (Liverpool
531 University, UK) on an Illumina HiSeq 2500 with SBS V4 chemistry. Raw sequencing reads
532 obtained from strain CVO and *S. denitrificans* transcriptomes have been deposited at NCBI's
533 SRA under the accession numbers PRJNA482764 and PRJNA504592, respectively.

534 Analysis of differentially expressed genes was conducted using CLC Genomic
535 Workbench (v. 10.1.1; Qiagen, UK). After demultiplexing and adapter removal, reads were
536 quality trimmed and mapped to their respective reference genomes (see supplementary methods
537 for further details). Read counts were normalized for gene length and total library size to
538 generate normalized FPKM (fragments mapped per kilobase per million reads) expression
539 values (Mortazavi *et al.*, 2008).

Empirical differential gene expression (DGE) analysis was conducted in CLC Genomic Workbench, which implements the 'Exact Test' to estimate negative binomial dispersion as previously described (Robinson and Smyth, 2008). The DGE analysis either compared gene expression during the biogenic elemental S^0 oxidation phase with the expression during sulfide oxidation phase (for both strains), or with active thiosulfate oxidation (only for *S. denitrificans*). DGE significance was assessed using the CLC implemented Gaussian-based *t*-test to perform a two-group comparison, with false discovery rate (FDR) correction applied to the original *p*-values based on the method described by Benjamini and Hochberg (1995). A fold change ≥ 1.5 or ≤ -1.5 and FDR corrected *p*-values <0.01 were used as a threshold for significant differential expression.

Nucleotide and protein sequence analysis

Nucleotide and amino acid sequences were retrieved from Genbank and the Integrated Microbial Genomes and Metagenomes (IMG/M) databases (Clark *et al.*, 2016; Chen *et al.*, 2017). Completeness of assembled genomes and metagenomes was assessed with the CheckM software package (Parks *et al.*, 2015). Structural and topological predictions of outer membrane proteins were performed with amino acid sequences via the web-based software BOCTOPUS2, PRED-TMBB2 and Phyre2 (Kelley *et al.*, 2015; Hayat *et al.*, 2016; Tsirigos *et al.*, 2016).

ACKNOWLEDGEMENT

This work was supported by an EU Marie Skłodowska Curie Fellowship (660401) to SL and research grants from the UK Engineering & Physical Sciences Research Council (EP/J002259/1, EP/L001942/1 and EP/K039083/1) and ExxonMobil Upstream Research Company (EM09030) to CRJH. We are grateful to Tim Ferdelman for supporting the sulfur compound analysis at the Max-Planck Institute for Marine Microbiology. We thank Demelza Menendez Vega and David Early for their technical support. The authors declare no conflict of interest.

566

567 **TABLE AND FIGURE LEGENDS**

568

569 Table 1 Genome information from *Sulfurimonas* sp. strain CVO compared to other sequenced
570 *Sulfurimonas* spp.

571

572 Table 2 Overview of differential gene expression for *Sulfurimonas* sp. strain CVO and
573 *Sulfurimonas denitrificans* DSM 1251.

574

575 Figure 1 Profiles of formation and consumption of sulfur species during anaerobic growth in
576 the presence of sulfide and excess nitrate by A) *Sulfurimonas* sp. strain CVO or B) *Sulfurimonas*
577 *denitrificans* DSM 1251. The error bars indicate the standard deviation between triplicate
578 cultures. Sterile control experiments can be found in Figure S1. H_2S, sulfide; S^0, zero-valent
579 elemental sulfur; SO_3^{2-}, sulfite; $S_2O_3^{2-}$, thiosulfate; sulfate, SO_4^{2-}. Sulfide and S^0 oxidation
580 phases are shaded in grey and yellow, respectively.

581

582 Figure 2 Genome comparison of *Sulfurimonas* sp. strain CVO and *Sulfurimonas denitrificans*
583 DSM 1251 showing abundances of clusters of orthologous genes (COGs).

584

585 Figure 3 Expression of homologous genes related to sulfur metabolism in A) *Sulfurimonas* sp.
586 strain CVO or B) *Sulfurimonas denitrificans* DSM 1251 during sulfide or biogenic elemental
587 sulfur (S^0) oxidation phases (see arrows in Fig. 1). Gene names are indicated underneath the
588 panels, and their functional categories are indicated above the panels. Normalized gene
589 expression is plotted as fragments per kilobase and million reads (FPKM). Error bars indicate
590 standard deviation from triplicate cultures. Significant changes in gene expression between the
591 S^0 oxidation and sulfide oxidation phase as determined by differential gene expression analysis

592 are shown above the gene names. In some cases, due to the absence of genes in the respective
593 genome transcripts were not detected (ND). Gene annotation – Sulfide quinone oxidoreductases
594 (SQR): *sqrB* = CVO_09655, Suden_0619, *sqrC* = Suden_1879, *sqrD* = CVO_06770,
595 Suden_0619, *sqrF* = CVO_05505; sulfur oxidation (SOX) complex subunits: *soxX* =
596 Suden_0260, *soxY1* = Suden_0261, *soxZ1* = Suden_0262, *soxA* = Suden_0263, *soxB* =
597 Suden_0264, *soxH* = CVO_09775, Suden_2056, *soxZ2* = CVO_09770, Suden_2057, *soxY2* =
598 CVO_09765, Suden_2058, *soxD* = CVO_09760, Suden_2059, *soxC* = CVO_09755,
599 Suden_2060; polysulfide reductase subunits: *psrB1* = CVO_07280, Suden_0498, *psrC1* =
600 CVO_07275, Suden_0499, *psrA1* = CVO_07270, Suden_0500, *psrA2* = CVO_09640, *psrB2* =
601 CVO_09635, *psrC2*= CVO_09630.
602
603 Figure 4 SOX gene clusters in the genomes of A) *Sulfurimonas* sp. strain CVO and B)
604 *Sulfurimonas denitrificans*. The scale bar represents nucleotide position in the respective
605 genomes. C) Distribution of genes related to sulfur metabolism in cultured isolate genomes and
606 metagenome-assembled genomes (MAGs) of *Sulfurimonas* spp.
607
608 Figure 5 Expression of homologous genes related to cell surface proteins in A) *Sulfurimonas*
609 sp. strain CVO or B) *Sulfurimonas denitrificans* DSM 1251 during sulfide or biogenic
610 elemental sulfur (S^0) oxidation phases (see arrows in Fig. 1). Gene names are indicated
611 underneath the panels, and their functional categories are indicated above the panels.
612 Normalized gene expression is plotted as fragments per kilobase and million reads (FPKM).
613 Error bars indicate standard deviation from triplicate cultures. Significant changes in gene
614 expression between the S^0 oxidation and sulfide oxidation phase as determined by differential
615 gene expression analysis are shown above the gene names. In some cases, due to the absence
616 of genes in the respective genome transcripts were not detected (ND). Gene annotation – Outer
617 membrane proteins: OmpA-like = CVO_00160, Suden_2018, OprD-like = CVO_00715,

_02730, _06365, Suden_1917, _1456, _0265; type IV general secretion proteins: PilC-like = CVO_03020, Suden_1388, PilB-like = CVO_03025, Suden_1387, PilQ-like = CVO_3045, Suden_1384, PilO-like = CVO_03055, Suden_1382; type IV pilus twitching motility protein: PilT-like = CVO_03705, _07430, Suden_1251; putative pilin precursors = CVO_07025, _07710, _07715, 07915, 07920, Suden_0572, _0410, _0409, _0367, _0366; type I secretion system: TolC family outer membrane protein = CVO_05415, ATPase = CVO_05420, membrane fusion protein = CVO_05425; DNA-binding response regulator = CVO_05430; cadherin domain-containing protein = CVO_05440, RTX (repeats in toxin) family proteins = CVO_05445, Suden_1200. *Orthologous gene.

Figure 6 Expression of homologous genes related to the flagellar apparatus in A) *Sulfurimonas* sp. strain CVO and B) *Sulfurimonas denitrificans* DSM 1251 during sulfide or biogenic elemental sulfur (S^0) oxidation phases (see arrows in Fig. 1). Gene names are indicated underneath the panels, and their functional categories are indicated above the panels. Normalized gene expression is plotted as fragments per kilobase and million reads (FPKM). Error bars indicate standard deviation from triplicate cultures. Significant changes in gene expression between the S^0 oxidation and sulfide oxidation phase as determined by differential gene expression analysis are shown above the gene names. In some cases, due to the absence of genes in the respective genome transcripts were not detected (ND). Gene annotation – flagellar hook-length control protein: *fliK* = Suden_0029; flagellar hook assembly protein: flgD = Suden_0030; flagellar hook-basal body protein: Suden_0031; flagellar hook protein: *flgE* = Suden_0032; flagellin and related hook-associated protein: Suden_0172, Suden_0173; flagellar capping protein: *fliD* = Suden_0202; flagellar biosynthetic protein: *fliS* = Suden_0203; flagellar hook-basal body complex protein: *fliE* = Suden_0363; flagellar basal-body rod protein: *flgC* = Suden_0364; Flagellar M-ring protein: *fliF* = CVO_07390, Suden_0472; flagellar motor switch protein: *fliG* = CVO_07385, Suden_0473; flagellar basal body P-ring protein: *flgI* =

644 Suden_0562; flagellar hook-associated protein: *flgK* = Suden_0566; flagellar motor switch
645 protein: *fliM* = CVO_06455, Suden_0707; flagellar motor switch protein: *fliN* = CVO_06450,
646 Suden_0708; flagellar basal body L-ring protein: *flgH* = Suden_0733; flagellar basal body
647 associated protein: *fliL* = Suden_0840; flagellin and related hook-associated protein:
648 Suden_1037; flagellar basal-body rod protein: *flgG* = Suden_1103; flagellar hook-basal body
649 protein: Suden_1104.
650
651 **SUPPORTING INFORMATION**
652 Figure S1 Formation and consumption of sulfur and nitrogen species during nitrate-mediated
653 oxidation of thiosulfate (A), biogenic zero-valent sulfur (B and C) or sulfide (D and E) in
654 *Sulfurimonas* cultures (left panel) and respective sterile controls (right panel). *Sulfurimonas*
655 *denitrificans* DSM 1251 (A and C) and *Sulfurimonas* sp. strain CVO (B).
656
657 Figure S2 Amounts of RNA extracted from cultures of *Sulfurimonas* sp. strain CVO or
658 *Sulfurimonas denitrificans* DSM 1251 when cultivated with different sulfur substrates and
659 nitrate as electron donor and acceptor (see Fig. 1 and Fig. S1).
660
661 Figure S3 Distribution of raw counts of mapped reads in each replicate across the
662 transcriptomes of A) *Sulfurimonas* sp. strain CVO and B) *Sulfurimonas denitrificans* DSM
663 1251. The box shows the median of the 1st quartile (lower line) and 3rd quartile (upper line),
664 while the middle line represents the overall median of the data set. The whiskers indicate upper
665 and lower limits of the data and outliers are represented by the filled circles.
666
667 Figure S4 Overall expression of clusters of orthologous genes (COGs) in A) *Sulfurimonas* sp.
668 strain CVO and B) *Sulfurimonas denitrificans* DSM 1251 during sulfide, biogenic zero-valent
669 sulfur (S^0) or thiosulfate oxidation phases. Normalized gene expression is shown as fragments

per kilobase and million reads (FPKM). Error bars indicate standard deviation from triplicate cultures.

Figure S5 Relationship of sulfide quinone oxidoreductases (SQR) protein sequences from *Sulfurimonas denitrificans* DSM 1251 and *Sulfurimonas* sp. strain CVO with proteins from other bacteria and archaea. Amino acid sequences were derived from the non-redundant protein database at NCBI and accession numbers are shown in brackets. Different SQR subtypes are marked according to previous classifications (Marcia *et al.*, 2010; Gregersen *et al.*, 2011). FCC: Flavocytochrome c sulfide dehydrogenase.

Figure S6 Visualization of cross-mapping reads obtained from sequencing DNA or RNA from strain CVO onto the genome of *Sulfurimonas denitrificans* DSM 1251. A) Genome track with coding sequences marked, B) mapping of Illumina MiSeq reads from DNA of strain CVO C) mapping of Illumina HiSeq reads from RNA of strain CVO. Zoom-in to the D) *soxXY$_1$Z$_1$AB* genes or E) *soxCDY$_2$Z$_2$H* genes.

Figure S7 Scanning electron micrographs of zero-valent elemental sulfur particles retrieved from cultures of *Sulfurimonas* sp. strain CVO (A-D), *Sulfurimonas denitrificans* DSM 1251 (E-H). The arrows indicate biofilm covered (solid line) or free surfaces (dashed line).

Figure S8 Proposed model for the oxidation of SoxY-bound sulfur and formation of sulfite in *Sulfurimonas* sp. strain CVO. Sulfite is proposed to then abiotically react with either zero-valent elemental sulfur or polysulfides to form thiosulfate. The activation mechanism of zero-valent sulfur and the hydrolysis steps that release sulfate or sulfite are currently unknown and marked with a question mark (?).

Table S1 Summary of differential gene expression parameters for cultures of *Sulfurimonas* sp. CVO and *Sulfurimonas denitrificans*.

Table S2 Information of metagenome-assembled genomes (MAG) of Sulfurimonas spp. from different habitats shown in Figure 4 of the main manuscript.

REFERENCE

Anantharaman, K., Brown, C.T., Hug, L.A., Sharon, I., Castelle, C.J., Probst, A.J., et al. (2016) Thousands of Microbial Genomes Shed Light on Interconnected Biogeochemical Processes in an Aquifer System. *Nat Commun* **7**: 13219.

Bankevich, A., Nurk, S., Antipov, D., Gurevich, A.A., Dvorkin, M., Kulikov, A.S., et al. (2012) SPAdes: A New Genome Assembly Algorithm and Its Applications to Single-Cell Sequencing. *J Comput Biol* **19**: 455–477.

Barken, K.B., Pamp, S.J., Yang, L., Gjermansen, M., Bertrand, J.J., Klausen, M., et al. (2008) Roles of Type IV Pili, Flagellum-Mediated Motility and Extracellular DNA in the Formation of Mature Multicellular Structures in *Pseudomonas aeruginosa* Biofilms. *Environ Microbiol* **10**: 2331–2343.

Benjamini, Y. and Hochberg, Y. (1995) Controlling the False Discovery Rate: A Practical and Powerful Approach to Multiple Testing. *J R Stat Soc Ser B Methodol* **57**: 289–300.

Berg, J.S., Schwedt, A., Kreutzmann, A.-C., Kuypers, M.M.M., and Milucka, J. (2014) Polysulfides as Intermediates in the Oxidation of Sulfide to Sulfate by *Beggiatoa* spp. *Appl Environ Microbiol* **80**: 629–636.

Bødtker, G., Thorstenson, T., Lillebø, B.-L.P., Thorbjørnsen, B.E., Ulvøen, R.H., Sunde, E., and Torsvik, T. (2008) The Effect of Long-Term Nitrate Treatment on SRB Activity, Corrosion Rate and Bacterial Community Composition in Offshore Water Injection Systems. *J Ind Microbiol Biotechnol* **35**: 1625–1636.

722 Boutet, E., Lieberherr, D., Tognolli, M., Schneider, M., and Bairoch, A. (2007)
723 UniProtKB/Swiss-Prot. *Methods Mol Biol Clifton NJ* **406**: 89–112.
724 Brune, D.C. (1989) Sulfur Oxidation by Phototrophic Bacteria. *Biochim Biophys Acta BBA -*
725 *Bioenerg* **975**: 189–221.
726 Buonfiglio, V., Polidoro, M., Flora, L., Citro, G., Valenti, P., and Orsi, N. (1993)
727 Identification of Two Outer Membrane Proteins Involved in the Oxidation of Sulphur
728 Compounds in *Thiobacillus ferrooxidans*. *FEMS Microbiol Rev* **11**: 43–50.
729 Cai, L., Shao, M.-F., and Zhang, T. (2014) Non-Contiguous Finished Genome Sequence and
730 Description of *Sulfurimonas hongkongensis* sp. nov., a Strictly Anaerobic
731 Denitrifying, Hydrogen- and Sulfur-Oxidizing Chemolithoautotroph Isolated from
732 Marine Sediment. *Stand Genomic Sci* **9**: 1302.
733 Callbeck, C.M., Lavik, G., Ferdelman, T.G., Fuchs, B., Gruber-Vodicka, H.R., Hach, P.F., et
734 al. (2018) Oxygen Minimum Zone Cryptic Sulfur Cycling Sustained by Offshore
735 Transport of Key Sulfur Oxidizing Bacteria. *Nat Commun* **9**: 1729.
736 Camacho, C., Coulouris, G., Avagyan, V., Ma, N., Papadopoulos, J., Bealer, K., and Madden,
737 T.L. (2009) BLAST+: Architecture and Applications. *BMC Bioinformatics* **10**: 421.
738 Carlson, H.K. and Hubert, C.R.J. (2019) Mechanisms and Monitoring of Oil Reservoir
739 Souring Control by Nitrate or Perchlorate Injection. In, McGenity,T.J. (ed), *Microbial*
740 *Communities Utilizing Hydrocarbons and Lipids: Members, Metagenomics and*
741 *Ecophysiology*, Handbook of Hydrocarbon and Lipid Microbiology. Cham: Springer
742 International Publishing, pp. 1–25.
743 Chen, I.-M.A., Markowitz, V.M., Chu, K., Palaniappan, K., Szeto, E., Pillay, M., et al. (2017)
744 IMG/M: Integrated Genome and Metagenome Comparative Data Analysis System.
745 *Nucleic Acids Res* **45**: D507–D516.
746 Chen, L., Ren, Y., Lin, Jianqun, Liu, X., Pang, X., and Lin, Jianqiang (2012)
747 *Acidithiobacillus caldus* Sulfur Oxidation Model Based on Transcriptome Analysis

748 between the Wild Type and Sulfur Oxygenase Reductase Defective Mutant. *PLOS*
749 *ONE* **7**: e39470.
750 Clark, K., Karsch-Mizrachi, I., Lipman, D.J., Ostell, J., and Sayers, E.W. (2016) GenBank.
751 *Nucleic Acids Res* **44**: D67–D72.
752 Cord-Ruwisch, R. (1985) A Quick Method for the Determination of Dissolved and
753 Precipitated Sulfides in Cultures of Sulfate-Reducing Bacteria. *J Microbiol Methods*
754 **4**: 33–36.
755 Corre, E., Reysenbach, A.L., and Prieur, D. (2001) Epsilon-Proteobacterial Diversity from a
756 Deep-Sea Hydrothermal Vent on the Mid-Atlantic Ridge. *FEMS Microbiol Lett* **205**:
757 329–335.
758 Craig, L., Forest, K.T., and Maier, B. (2019) Type IV Pili: Dynamics, Biophysics and
759 Functional Consequences. *Nat Rev Microbiol* **17**: 429–440.
760 Dahle, H., Roalkvam, I., Thorseth, I.H., Pedersen, R.B., and Steen, I.H. (2013) The Versatile
761 *in situ* Gene Expression of an *Epsilonproteobacteria*-Dominated Biofilm from a
762 Hydrothermal Chimney. *Environ Microbiol Rep* **5**: 282–290.
763 Finster, K., Liesack, W., and Thamdrup, B. (1998) Elemental Sulfur and Thiosulfate
764 Disproportionation by *Desulfocapsa sulfoexigens* sp. nov., a New Anaerobic
765 Bacterium Isolated from Marine Surface Sediment. *Appl Environ Microbiol* **64**: 119–
766 125.
767 Fraiberg, M., Borovok, I., Weiner, R.M., Lamed, R., and Bayer, E.A. (2012) Bacterial
768 Cadherin Domains as Carbohydrate Binding Modules: Determination of Affinity
769 Constants to Insoluble Complex Polysaccharides. *Methods Mol Biol Clifton NJ* **908**:
770 109–118.
771 Friedrich, C.G., Rother, D., Bardischewsky, F., Quentmeier, A., and Fischer, J. (2001)
772 Oxidation of Reduced Inorganic Sulfur Compounds by Bacteria: Emergence of a
773 Common Mechanism? *Appl Environ Microbiol* **67**: 2873–2882.

774 Frigaard, N.-U. and Dahl, C. (2009) Sulfur Metabolism in Phototrophic Sulfur Bacteria. In,
775 Poole, R.K. (ed), *Advances in Microbial Physiology*. Academic Press, pp. 103–200.
776 Gevertz, D., Telang, A.J., Voordouw, G., and Jenneman, G.E. (2000) Isolation and
777 Characterization of Strains CVO and FWKO B, Two Novel Nitrate-Reducing,
778 Sulfide-Oxidizing Bacteria Isolated from Oil Field Brine. *Appl Environ Microbiol* **66**:
779 2491–2501.
780 Ghosh, W. and Dam, B. (2009) Biochemistry and Molecular Biology of Lithotrophic Sulfur
781 Oxidation by Taxonomically and Ecologically Diverse Bacteria and Archaea. *FEMS*
782 *Microbiol Rev* **33**: 999–1043.
783 Gittel, A., Kofoed, M.V.W., Sørensen, K.B., Ingvorsen, K., and Schramm, A. (2012)
784 Succession of *Deferribacteres* and *Epsilonproteobacteria* Through a Nitrate-Treated
785 High-Temperature Oil Production Facility. *Syst Appl Microbiol* **35**: 165–174.
786 Glaubitz, S., Labrenz, M., Jost, G., and Jürgens, K. (2010) Diversity of Active
787 Chemolithoautotrophic Prokaryotes in the Sulfidic Zone of a Black Sea Pelagic
788 Redoxcline as Determined by rRNA-Based Stable Isotope Probing. *FEMS Microbiol*
789 *Ecol* **74**: 32–41.
790 Götz, F., Pjevac, P., Markert, S., McNichol, J., Becher, D., Schweder, T., et al. (2019)
791 Transcriptomic and Proteomic Insight into the Mechanism of Cyclooctasulfur- Versus
792 Thiosulfate-Oxidation by the Chemolithoautotroph *Sulfurimonas denitrificans*.
793 *Environ Microbiol* **21**: 244–258.
794 Grabarczyk, D.B. and Berks, B.C. (2017) Intermediates in the Sox Sulfur Oxidation Pathway
795 are Bound to a Sulfane Conjugate of the Carrier Protein SoxYZ. *PLOS ONE* **12**:
796 e0173395.
797 Gregersen, L.H., Bryant, D.A., and Frigaard, N.-U. (2011) Mechanisms and Evolution of
798 Oxidative Sulfur Metabolism in Green Sulfur Bacteria. *Front Microbiol* **2**: 116.

799 Griesbeck, C., Schütz, M., Schödl, T., Bathe, S., Nausch, L., Mederer, N., et al. (2002)
800 Mechanism of Sulfide-Quinone Reductase Investigated Using Site-Directed
801 Mutagenesis and Sulfur Analysis. *Biochemistry* **41**: 11552–11565.
802 Grote, J., Jost, G., Labrenz, M., Herndl, G.J., and Jürgens, K. (2008) *Epsilonproteobacteria*
803 Represent the Major Portion of Chemoautotrophic Bacteria in Sulfidic Waters of
804 Pelagic Redoxclines of the Baltic and Black Seas. *Appl Environ Microbiol* **74**: 7546–
805 7551.
806 Grote, J., Schott, T., Bruckner, C.G., Glockner, F.O., Jost, G., Teeling, H., et al. (2012)
807 Genome and Physiology of a Model Epsilonproteobacterium Responsible for Sulfide
808 Detoxification in Marine Oxygen Depletion Zones. *Proc Natl Acad Sci U S A* **109**:
809 506–510.
810 Haft, D.H., DiCuccio, M., Badretdin, A., Brover, V., Chetvernin, V., O'Neill, K., et al. (2018)
811 RefSeq: An Update on Prokaryotic Genome Annotation and Curation. *Nucleic Acids*
812 *Res* **46**: D851–D860.
813 Han, Y. and Perner, M. (2016) Sulfide Consumption in *Sulfurimonas denitrificans* and
814 Heterologous Expression of its Three SQR Homologs. *J Bacteriol* JB.01021-15.
815 Han, Y. and Perner, M. (2015) The Globally Widespread Genus *Sulfurimonas*: Versatile
816 Energy Metabolisms and Adaptations to Redox Clines. *Microb Physiol Metab* 989.
817 Handley, K.M., VerBerkmoes, N.C., Steefel, C.I., Williams, K.H., Sharon, I., Miller, C.S., et
818 al. (2013) Biostimulation Induces Syntrophic Interactions that Impact C, S and N
819 Cycling in a Sediment Microbial Community. *ISME J* **7**: 800–816.
820 Hayat, S., Peters, C., Shu, N., Tsirigos, K.D., and Elofsson, A. (2016) Inclusion of Dyad-
821 Repeat Pattern Improves Topology Prediction of Transmembrane β-Barrel Proteins.
822 *Bioinforma Oxf Engl* **32**: 1571–1573.

Hensen, D., Sperling, D., Trüper, H.G., Brune, D.C., and Dahl, C. (2006) Thiosulphate Oxidation in the Phototrophic Sulphur Bacterium *Allochromatium vinosum*. *Mol Microbiol* **62**: 794–810.

Hinsa, S.M., Espinosa-Urgel, M., Ramos, J.L., and O'Toole, G.A. (2003) Transition from Reversible to Irreversible Attachment During Biofilm Formation by *Pseudomonas fluorescens* WCS365 Requires an ABC Transporter and a Large Secreted Protein. *Mol Microbiol* **49**: 905–918.

Howarth, R.W. (1984) The Ecological Significance of Sulfur in the Energy Dynamics of Salt Marsh and Coastal Marine Sediments. *Biogeochemistry* **1**: 5–27.

Hubert, C., Nemati, M., Jenneman, G., and Voordouw, G. (2003) Containment of Biogenic Sulfide Production in Continuous Up-Flow Packed-Bed Bioreactors with Nitrate or Nitrite. *Biotechnol Prog* **19**: 338–345.

Hubert, C., Nemati, M., Jenneman, G., and Voordouw, G. (2005) Corrosion Risk Associated with Microbial Souring Control Using Nitrate or Nitrite. *Appl Microbiol Biotechnol* **68**: 272–282.

Hubert, C.R.J., Oldenburg, T.B.P., Fustic, M., Gray, N.D., Larter, S.R., Penn, K., et al. (2012) Massive Dominance of *Epsilonproteobacteria* in Formation Waters from a Canadian Oil Sands Reservoir Containing Severely Biodegraded Oil. *Environ Microbiol* **14**: 387–404.

Jarrell, K.F., Stark, M., Nair, D.B., and Chong, J.P.J. (2011) Flagella and Pili are Both Necessary for Efficient Attachment of *Methanococcus maripaludis* to Surfaces. *FEMS Microbiol Lett* **319**: 44–50.

Jewell, T.N.M., Karaoz, U., Brodie, E.L., Williams, K.H., and Beller, H.R. (2016) Metatranscriptomic Evidence of Pervasive and Diverse Chemolithoautotrophy Relevant to C, S, N and Fe Cycling in a Shallow Alluvial Aquifer. *ISME J* **10**: 2106–2117.

Jørgensen, B.B. (1982) Ecology of the Bacteria of the Sulphur Cycle with Special Reference to Anoxic—Oxic Interface Environments. *Phil Trans R Soc Lond B* **298**: 543–561.

Jørgensen, B.B. (1990a) A Thiosulfate Shunt in the Sulfur Cycle of Marine Sediments. *Science* **249**: 152–154.

Jørgensen, B.B. (1990b) The Sulfur Cycle of Freshwater Sediments: Role of Thiosulfate. *Limnol Oceanogr* **35**: 1329–1342.

Kalmokoff, M., Lanthier, P., Tremblay, T.-L., Foss, M., Lau, P.C., Sanders, G., et al. (2006) Proteomic Analysis of *Campylobacter jejuni* 11168 Biofilms Reveals a Role for the Motility Complex in Biofilm Formation. *J Bacteriol* **188**: 4312–4320.

Kelley, L.A., Mezulis, S., Yates, C.M., Wass, M.N., and Sternberg, M.J. (2015) The Phyre2 Web Portal for Protein Modelling, Prediction and Analysis. *Nat Protoc* **10**: 845–858.

Kelly, D.P., Shergill, J.K., Lu, W.-P., and Wood, A.P. (1997) Oxidative Metabolism of Inorganic Sulfur Compounds by Bacteria. *Antonie Van Leeuwenhoek* **71**: 95–107.

Kletzin, A. (1989) Coupled Enzymatic Production of Sulfite, Thiosulfate, and Hydrogen Sulfide from Sulfur: Purification and Properties of a Sulfur Oxygenase Reductase from the Facultatively Anaerobic Archaebacterium *Desulfurolobus ambivalens*. *J Bacteriol* **171**: 1638–1643.

Lahme, S., Enning, D., Callbeck, C.M., Vega, D.M., Curtis, T.P., Head, I.M., and Hubert, C.R.J. (2019) Metabolites of an Oil Field Sulfide-Oxidizing, Nitrate-Reducing *Sulfurimonas* sp. Cause Severe Corrosion. *Appl Env Microbiol* **85**: e01891-18.

Lenk, S., Arnds, J., Zerjatke, K., Musat, N., Amann, R., and Mussmann, M. (2011) Novel Groups of *Gammaproteobacteria* Catalyse Sulfur Oxidation and Carbon Fixation in a Coastal, Intertidal Sediment. *Environ Microbiol* **13**: 758–774.

Mangold, S., Valdés, J., Holmes, D.S., and Dopson, M. (2011) Sulfur Metabolism in the Extreme Acidophile *Acidithiobacillus caldus*. *Front Microbiol* **2**: 17.

874 Marcia, M., Ermler, U., Peng, G., and Michel, H. (2010) A New Structure-Based
875 Classification of Sulfide:Quinone Oxidoreductases. *Proteins* **78**: 1073–1083.
876 Meier, D.V., Pjevac, P., Bach, W., Hourdez, S., Girguis, P.R., Vidoudez, C., et al. (2017)
877 Niche Partitioning of Diverse Sulfur-Oxidizing Bacteria at Hydrothermal Vents. *ISME*
878 *J* **11**: 1545–1558.
879 Minamino, T. and Imada, K. (2015) The Bacterial Flagellar Motor and its Structural
880 Diversity. *Trends Microbiol* **23**: 267–274.
881 Mitchell, A.L., Attwood, T.K., Babbitt, P.C., Blum, M., Bork, P., Bridge, A., et al. (2019)
882 InterPro in 2019: Improving Coverage, Classification and Access to Protein Sequence
883 Annotations. *Nucleic Acids Res* **47**: D351–D360.
884 Mortazavi, A., Williams, B.A., McCue, K., Schaeffer, L., and Wold, B. (2008) Mapping and
885 Quantifying Mammalian Transcriptomes by RNA-Seq. *Nat Methods* **5**: 621–628.
886 Nemati, M., Jenneman, G.E., and Voordouw, G. (2001) Impact of Nitrate-Mediated Microbial
887 Control of Souring in Oil Reservoirs on the Extent of Corrosion. *Biotechnol Prog* **17**:
888 852–859.
889 Nishikawa, S., Shinzawa, N., Nakamura, K., Ishigaki, K., Abe, H., and Horiguchi, Y. (2016)
890 The *bvg*-Repressed Gene *brtA*, Encoding Biofilm-Associated Surface Adhesin, is
891 Expressed During Host Infection by *Bordetella bronchiseptica*. *Microbiol Immunol*
892 **60**: 93–105.
893 Ohmura, N., Tsugita, K., Koizumi, J.I., and Saika, H. (1996) Sulfur-Binding Protein of
894 Flagella of *Thiobacillus ferrooxidans*. *J Bacteriol* **178**: 5776–5780.
895 O'Toole, G.A. and Kolter, R. (1998) Flagellar and Twitching Motility are Necessary for
896 *Pseudomonas aeruginosa* Biofilm Development. *Mol Microbiol* **30**: 295–304.
897 Ottemann, K.M. and Lowenthal, A.C. (2002) *Helicobacter pylori* Uses Motility for Initial
898 Colonization and to Attain Robust Infection. *Infect Immun* **70**: 1984–1990.

899 Parks, D.H., Imelfort, M., Skennerton, C.T., Hugenholtz, P., and Tyson, G.W. (2015)
900 CheckM: Assessing the Quality of Microbial Genomes Recovered from Isolates,
901 Single Cells, and Metagenomes. *Genome Res* **25**: 1043–1055.
902 Pjevac, P., Kamyshny, A., Dyksma, S., and Mußmann, M. (2014) Microbial Consumption of
903 Zero-Valence Sulfur in Marine Benthic Habitats. *Environ Microbiol* **16**: 3416–3430.
904 Pjevac, P., Meier, D.V., Markert, S., Hentschker, C., Schweder, T., Becher, D., et al. (2018)
905 Metaproteogenomic Profiling of Microbial Communities Colonizing Actively Venting
906 Hydrothermal Chimneys. *Front Microbiol* **9**:.
907 Pratt, L.A. and Kolter, R. (1998) Genetic Analysis of *Escherichia coli* Biofilm Formation:
908 Roles of Flagella, Motility, Chemotaxis and Type I Pili. *Mol Microbiol* **30**: 285–293.
909 Probst, A.J., Ladd, B., Jarett, J.K., Geller-McGrath, D.E., Sieber, C.M.K., Emerson, J.B., et
910 al. (2018) Differential Depth Distribution of Microbial Function and Putative
911 Symbionts Through Sediment-Hosted Aquifers in the Deep Terrestrial Subsurface.
912 *Nat Microbiol* **3**: 328–336.
913 Ramírez, P., Guiliani, N., Valenzuela, L., Beard, S., and Jerez, C.A. (2004) Differential
914 Protein Expression during Growth of *Acidithiobacillus ferrooxidans* on Ferrous Iron,
915 Sulfur Compounds, or Metal Sulfides. *Appl Env Microbiol* **70**: 4491–4498.
916 Richter, L.V., Sandler, S.J., and Weis, R.M. (2012) Two Isoforms of *Geobacter*
917 *sulfurreducens* PilA Have Distinct Roles in Pilus Biogenesis, Cytochrome
918 Localization, Extracellular Electron Transfer, and Biofilm Formation. *J Bacteriol* **194**:
919 2551–2563.
920 Robinson, M.D. and Smyth, G.K. (2008) Small-Sample Estimation of Negative Binomial
921 Dispersion, with Applications to SAGE Data. *Biostat Oxf Engl* **9**: 321–332.
922 Rohwerder, T. and Sand, W. (2003) The Sulfane Sulfur of Persulfides is the Actual Substrate
923 of the Sulfur-Oxidizing Enzymes from *Acidithiobacillus* and *Acidiphilium* spp.
924 *Microbiology* **149**: 1699–1710.

925 Rother, D., Henrich, H.-J., Quentmeier, A., Bardischewsky, F., and Friedrich, C.G. (2001)
926 Novel Genes of the *sox* Gene Cluster, Mutagenesis of the Flavoprotein SoxF, and
927 Evidence for a General Sulfur-Oxidizing System in *Paracoccus pantotrophus* GB17. *J*
928 *Bacteriol* **183**: 4499–4508.
929 Rutherford, K., Parkhill, J., Crook, J., Horsnell, T., Rice, P., Rajandream, M.A., and Barrell,
930 B. (2000) Artemis: Sequence Visualization and Annotation. *Bioinforma Oxf Engl* **16**:
931 944–945.
932 Satchell, K.J.F. (2011) Structure and Function of MARTX Toxins and Other Large Repetitive
933 RTX Proteins. *Annu Rev Microbiol* **65**: 71–90.
934 Schaeffer, W.I., Holbert, P.E., and Umbreit, W.W. (1963) Attachment of *Thiobacillus*
935 *thiooxidans* to Sulfur Crystals. *J Bacteriol* **85**: 137–140.
936 Schütz, M., Maldener, I., Griesbeck, C., and Hauska, G. (1999) Sulfide-Quinone Reductase
937 from *Rhodobacter capsulatus*: Requirement for Growth, Periplasmic Localization, and
938 Extension of Gene Sequence Analysis. *J Bacteriol* **181**: 6516–6523.
939 Shartau, S.L.C., Yurkiw, M., Lin, S., Grigoryan, A.A., Lambo, A., Park, H.-S., et al. (2010)
940 Ammonium Concentrations in Produced Waters from a Mesothermic Oil Field
941 Subjected to Nitrate Injection Decrease Through Formation of Denitrifying Biomass
942 and Anammox Activity. *Appl Environ Microbiol* **76**: 4977–4987.
943 Sievert, S.M., Scott, K.M., Klotz, M.G., Chain, P.S.G., Hauser, L.J., Hemp, J., et al. (2008)
944 Genome of the Epsilonproteobacterial Chemolithoautotroph *Sulfurimonas*
945 *denitrificans*. *Appl Environ Microbiol* **74**: 1145–1156.
946 Sikorski, J., Munk, C., Lapidus, A., Ngatchou Djao, O.D., Lucas, S., Glavina Del Rio, T., et
947 al. (2010) Complete Genome Sequence of *Sulfurimonas autotrophica* Type Strain
948 (OK10). *Stand Genomic Sci* **3**: 194–202.

949 Steudel, R. (1996) Mechanism for the Formation of Elemental Sulfur from Aqueous Sulfide
950 in Chemical and Microbiological Desulfurization Processes. *Ind Eng Chem Res* **35**:
951 1417–1423.
952 Svensson, S.L., Pryjma, M., and Gaynor, E.C. (2014) Flagella-Mediated Adhesion and
953 Extracellular DNA Release Contribute to Biofilm Formation and Stress Tolerance of
954 *Campylobacter jejuni*. *PLOS ONE* **9**: e106063.
955 Takai, K., Suzuki, M., Nakagawa, S., Miyazaki, M., Suzuki, Y., Inagaki, F., and Horikoshi,
956 K. (2006) *Sulfurimonas paralvinellae* sp. nov., a Novel Mesophilic, Hydrogen- and
957 Sulfur-Oxidizing Chemolithoautotroph within the *Epsilonproteobacteria* Isolated
958 from a Deep-Sea Hydrothermal Vent Polychaete Nest, Reclassification of
959 *Thiomicrospira denitrificans* as *Sulfurimonas denitrificans* comb. nov. and Emended
960 Description of the Genus *Sulfurimonas*. *Int J Syst Evol Microbiol* **56**: 1725–1733.
961 Tatusova, T., DiCuccio, M., Badretdin, A., Chetvernin, V., Nawrocki, E.P., Zaslavsky, L., et
962 al. (2016) NCBI Prokaryotic Genome Annotation Pipeline. *Nucleic Acids Res* **44**:
963 6614–6624.
964 Telang, A.J., Ebert, S., Foght, J.M., Westlake, D., Jenneman, G.E., Gevertz, D., and
965 Voordouw, G. (1997) Effect of Nitrate Injection on the Microbial Community in an
966 Oil Field as Monitored by Reverse Sample Genome Probing. *Appl Environ Microbiol*
967 **63**: 1785–1793.
968 Telang, A.J., Jenneman, G.E., and Voordouw, G. (1999) Sulfur Cycling in Mixed Cultures of
969 Sulfide-Oxidizing and Sulfate- or Sulfur-Reducing Oil Field Bacteria. *Can J*
970 *Microbiol* **45**: 905–913.
971 Timmer-Ten Hoor, A. (1975) A New Type of Thiosulphate Oxidizing, Nitrate Reducing
972 Microorganism: *Thiomicrospira denitrificans* sp. nov. *Neth J Sea Res* **9**: 344–350.
973 Tommassen, J. (2010) Assembly of Outer-Membrane Proteins in Bacteria and Mitochondria.
974 *Microbiol Read Engl* **156**: 2587–2596.

975 Tsirigos, K.D., Elofsson, A., and Bagos, P.G. (2016) PRED-TMBB2: Improved Topology
976 Prediction and Detection of Beta-Barrel Outer Membrane Proteins. *Bioinforma Oxf*
977 *Engl* **32**: i665–i671.
978 Vigneron, A., Alsop, E.B., Lomans, B.P., Kyrpides, N.C., Head, I.M., and Tsesmetzis, N.
979 (2017) Succession in the Petroleum Reservoir Microbiome Through an Oil Field
980 Production Lifecycle. *ISME J* **11**: 2141–2154.
981 Vozza, N.F., Abdian, P.L., Russo, D.M., Mongiardini, E.J., Lodeiro, A.R., Molin, S., and
982 Zorreguieta, A. (2016) A *Rhizobium leguminosarum* CHDL- (Cadherin-Like-) Lectin
983 Participates in Assembly and Remodeling of the Biofilm Matrix. *Front Microbiol* **7**:.
984 Weissgerber, T., Dobler, N., Polen, T., Latus, J., Stockdreher, Y., and Dahl, C. (2013)
985 Genome-Wide Transcriptional Profiling of the Purple Sulfur Bacterium
986 *Allochromatium vinosum* DSM 180T during Growth on Different Reduced Sulfur
987 Compounds. *J Bacteriol* **195**: 4231–4245.
988 Wu, X., Pedersen, K., Edlund, J., Eriksson, L., Åström, M., Andersson, A.F., et al. (2017)
989 Potential for Hydrogen-Oxidizing Chemolithoautotrophic and diazotrophic
990 Populations to Initiate Biofilm Formation in Oligotrophic, Deep Terrestrial Subsurface
991 Waters. *Microbiome* **5**: 37.
992 Xia, Y., Lü, C., Hou, N., Xin, Y., Liu, J., Liu, H., and Xun, L. (2017) Sulfide Production and
993 Oxidation by Heterotrophic Bacteria under Aerobic Conditions. *ISME J* **11**: 2754–
994 2766.
995 Xin, Y., Liu, Honglei, Cui, F., Liu, Huaiwei, and Xun, L. (2016) Recombinant *Escherichia*
996 *coli* with Sulfide:Quinone Oxidoreductase and Persulfide Dioxygenase Rapidly
997 Oxidises Sulfide to Sulfite and Thiosulfate via a New Pathway. *Environ Microbiol* **18**:
998 5123–5136.
999 Zander, U., Faust, A., Klink, B.U., Sanctis, D. de, Panjikar, S., Quentmeier, A., et al. (2011)
1000 Structural Basis for the Oxidation of Protein-bound Sulfur by the Sulfur Cycle

Molybdohemo-Enzyme Sulfane Dehydrogenase SoxCD. *J Biol Chem* **286**: 8349–
8360.

Table 1

Organism	Isolation source	Accession No.	Genome size (Mbp)	%GC	Genes	rRNA operons	tRNA	Protein coding	Reference
***Sulfurimonas* sp. strain CVO**	**Terrestrial oil field produced water**	**CP033720**	**1.92**	**34.5**	**1957**	**4**	**43**	**1899**	**This study**
Sulfurimonas denitrificans DSM 1251	Coastal marine sediments	NC_007575	2.20	34.5	2196	4	44	2133	Sievert *et al.* 2008
Sulfurimonas autotrophica OK10	Deep-sea hydrothermal vent sediment	NC_014506	2.15	35.2	2204	4	43	2140	Sikorski *et al*. 2010
Sulfurimonas gotlandica GD1	Marine pelagic redoxcline	NZ_AFRZ01000001	2.95	33.6	2894	4	47	2817	Grote *et al.* 2012
Sulfurimonas hongkongensis AST-10	Coastal marine sediments	NZ_AUPZ00000000	2.30	34.9	2332	3	39	2290	Cai *et al.* 2014

Table 2

Organism	Transcripts detected [a]		Differentially abundant [c]	
	H_2S	Bio S^0	Increased	Decreased
Sulfurimonas sp. strain CVO	1832	1839	588	528
Sulfurimonas denitrificans DSM 1251	1949	2036 (1985)	612 (299)	534 (493)

[a] Transcripts detected refers to at least an expression value of 10 fragments per kilobase and million reads (FPKM).

[b] Highly expressed refers to an FPKM expression value ≥1000; values in parenthesis refers to thiosulfate grown cells.

[c] Differentially abundant refers to a fold change in FPKM of ≥ 1.5 or ≤ –1.5 during the biogenic zero-valent sulfur (Bio S^0) compared to the sulfide oxidation phase, as well as a false discovery rate corrected *p*-value ≤ 0.01; the value in parenthesis refers to a comparison of thiosulfate grown cells with cells during the Bio S^0 oxidation phase.

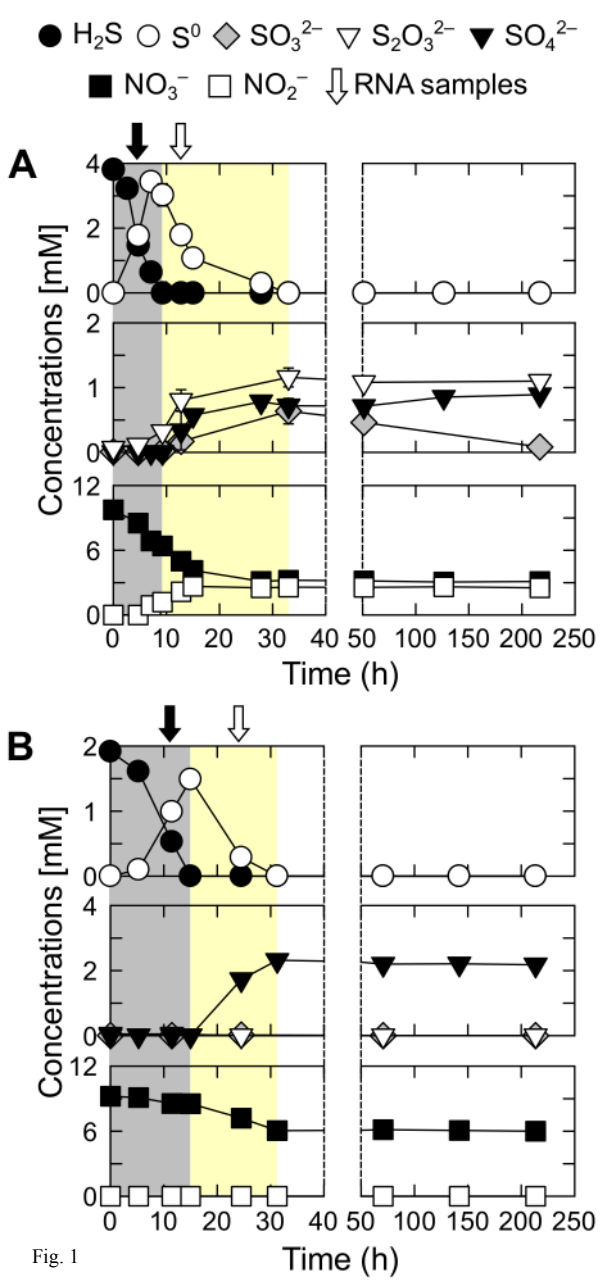
H2S
S0
SO3 2−
S2O3 2−
SO4 2−
NO3−
NO2−
RNA samples
A
B
Concentrations [mM]
Time (h)

Fig. 1

Sulfurimonas sp. strain CVO

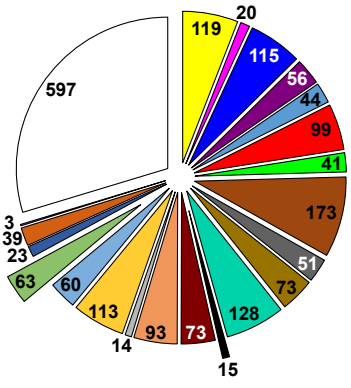

Sulfurimonas denitrificans

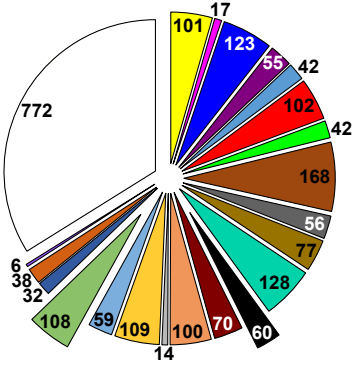

- Energy production and conversion (C)
- Cell cycle control, cell division, chromosome partitioning (D)
- Amino acid transport and metabolism (E)
- Nucleotide transport and metabolism (F)
- Carbohydrate transport and metabolism (G)
- Coenzyme transport and metabolism (H)
- Lipid transport and metabolism (I)
- Translation, ribosomal structure and biogenesis (J)
- Transcription (K)
- Replication, recombination and repair (L)
- Cell wall/membrane/envelope biogenesis (M)
- Cell motility (N)
- Posttranslational modification, protein turnover, chaperones (O)
- Inorganic ion transport and metabolism (P)
- Secondary metabolites biosynthesis, transport and catabolism (Q)
- General function prediction only (R)
- Function unknown (S)
- Signal transduction mechanisms (T)
- Intracellular trafficking, secretion and vesicular transport (U)
- Defense mechanisms (V)
- Mobilome: prophages, transposons (X)
- Protein coding genes w/o identified COG

Fig. 2

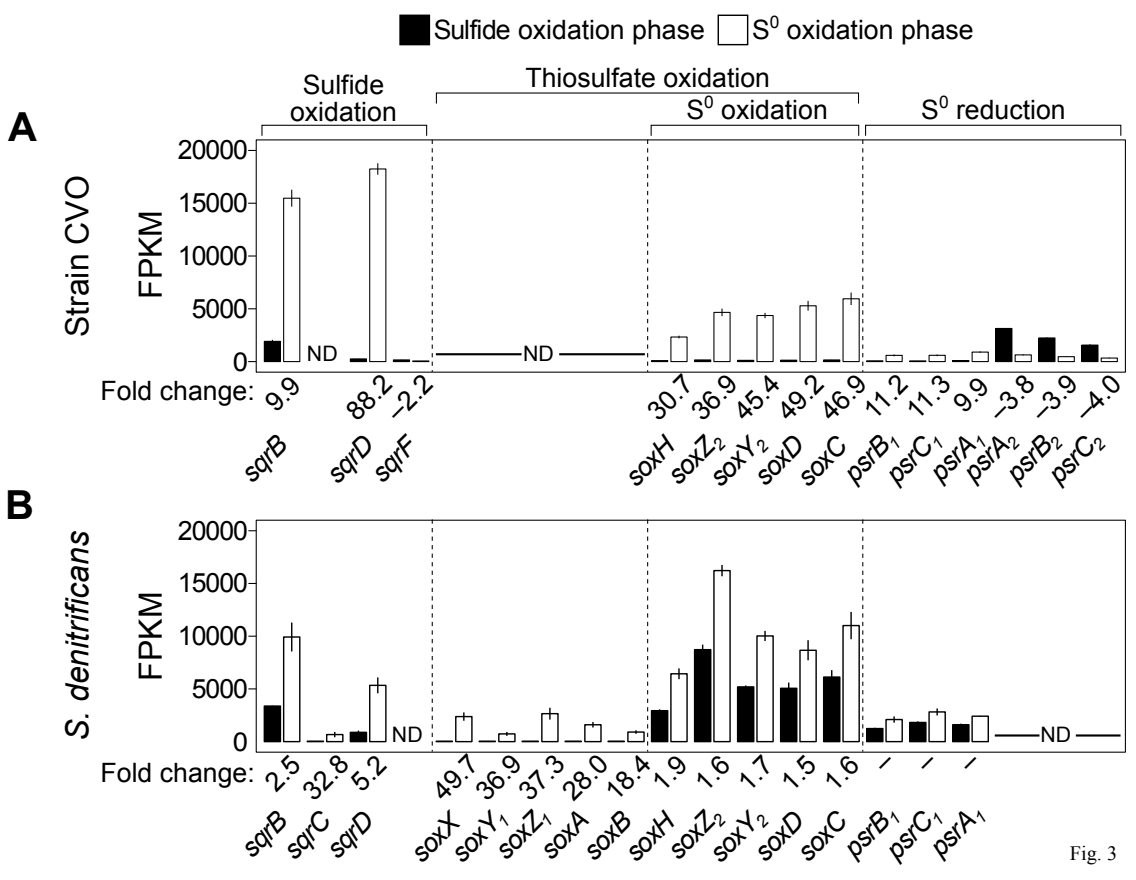
Sulfide oxidation phase
S0 oxidation phase
A
Strain CVO
Sulfide oxidation
Thiosulfate oxidation
S0 oxidation
S0 reduction
FPKM
20000
15000
10000
5000
0
ND
ND
Fold change:
9.9
88.2
−2.2
30.7
36.9
45.4
49.2
46.9
11.2
11.3
9.9
−3.8
−3.9
−4.0
sqrB
sqrD
sqrF
soxH
soxZ2
soxY2
soxD
soxC
psrB1
psrC1
psrA1
psrA2
psrB2
psrC2
B
S. denitrificans
FPKM
20000
15000
10000
5000
0
ND
ND
Fold change:
2.5
32.8
5.2
49.7
36.9
37.3
28.0
18.4
1.9
1.6
1.7
1.5
1.6
–
–
–
sqrB
sqrC
sqrD
soxX
soxY1
soxZ1
soxA
soxB
soxH
soxZ2
soxY2
soxD
soxC
psrB1
psrC1
psrA1

Fig. 3

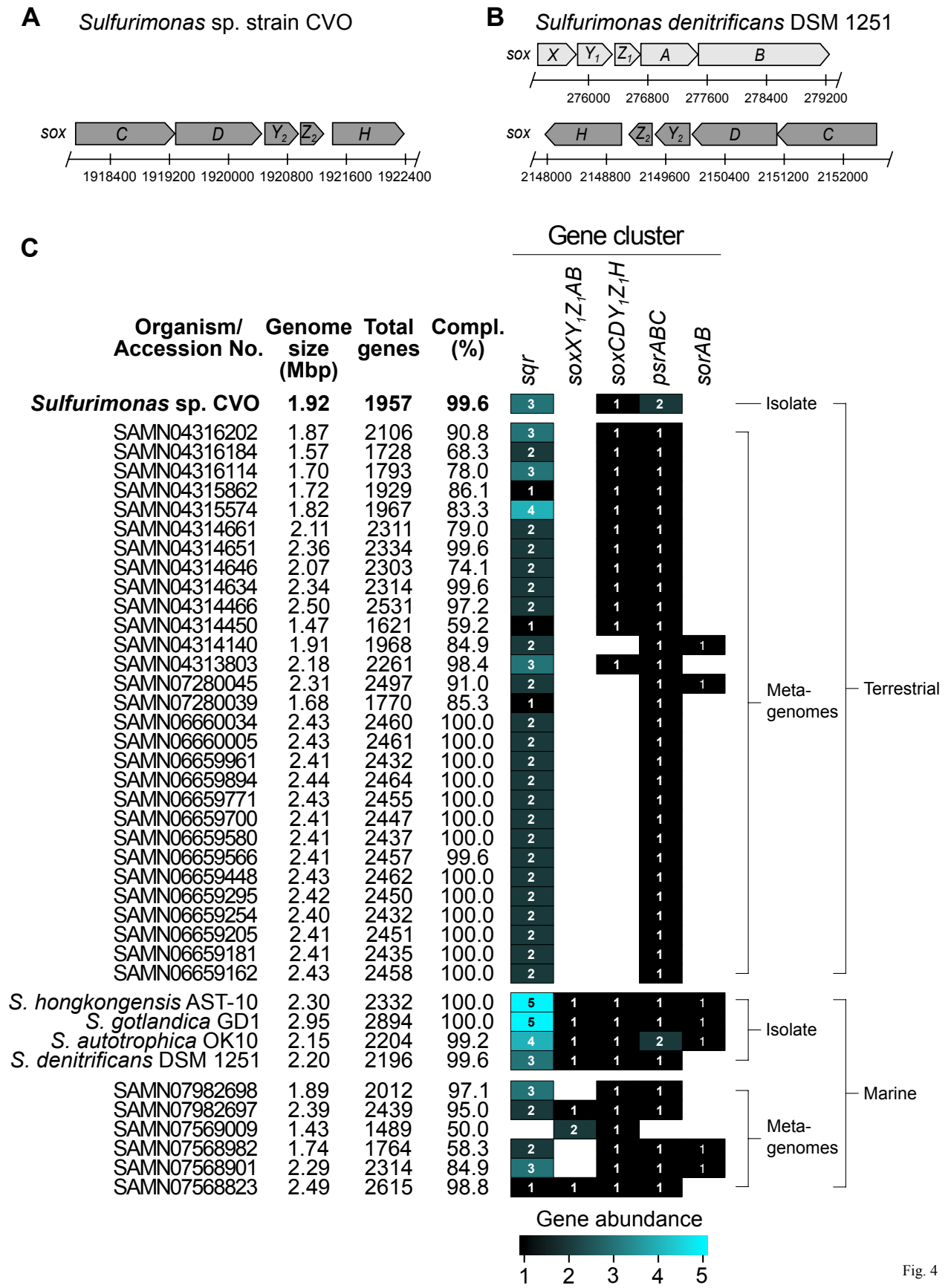
A
Sulfurimonas sp. strain CVO
sox
C
D
Y2
Z2
H
1918400 1919200 1920000 1920800 1921600 1922400
B
Sulfurimonas denitrificans DSM 1251
sox
X
Y1
Z1
A
B
276000 276800 277600 278400 279200
sox
H
Z2
Y2
D
C
2148000 2148800 2149600 2150400 2151200 2152000
C
Gene cluster
sqr
soxXY1Z1AB
soxCDY1Z1H
psrABC
sorAB
Organism/ Accession No.
Genome size (Mbp)
Total genes
Compl. (%)
Sulfurimonas sp. CVO 1.92 1957 99.6
SAMN04316202 1.87 2106 90.8
SAMN04316184 1.57 1728 68.3
SAMN04316114 1.70 1793 78.0
SAMN04315862 1.72 1929 86.1
SAMN04315574 1.82 1967 83.3
SAMN04314661 2.11 2311 79.0
SAMN04314651 2.36 2334 99.6
SAMN04314646 2.07 2303 74.1
SAMN04314634 2.34 2314 99.6
SAMN04314466 2.50 2531 97.2
SAMN04314450 1.47 1621 59.2
SAMN04314140 1.91 1968 84.9
SAMN04313803 2.18 2261 98.4
SAMN07280045 2.31 2497 91.0
SAMN07280039 1.68 1770 85.3
SAMN06660034 2.43 2460 100.0
SAMN06660005 2.43 2461 100.0
SAMN06659961 2.41 2432 100.0
SAMN06659894 2.44 2464 100.0
SAMN06659771 2.43 2455 100.0
SAMN06659700 2.41 2447 100.0
SAMN06659580 2.41 2437 100.0
SAMN06659566 2.41 2457 99.6
SAMN06659448 2.43 2462 100.0
SAMN06659295 2.42 2450 100.0
SAMN06659254 2.40 2432 100.0
SAMN06659205 2.41 2451 100.0
SAMN06659181 2.41 2435 100.0
SAMN06659162 2.43 2458 100.0
S. hongkongensis AST-10 2.30 2332 100.0
S. gotlandica GD1 2.95 2894 100.0
S. autotrophica OK10 2.15 2204 99.2
S. denitrificans DSM 1251 2.20 2196 99.6
SAMN07982698 1.89 2012 97.1
SAMN07982697 2.39 2439 95.0
SAMN07569009 1.43 1489 50.0
SAMN07568982 1.74 1764 58.3
SAMN07568901 2.29 2314 84.9
SAMN07568823 2.49 2615 98.8
Isolate
Meta-genomes
Terrestrial
Isolate
Meta-genomes
Marine
Gene abundance
1 2 3 4 5

Fig. 4

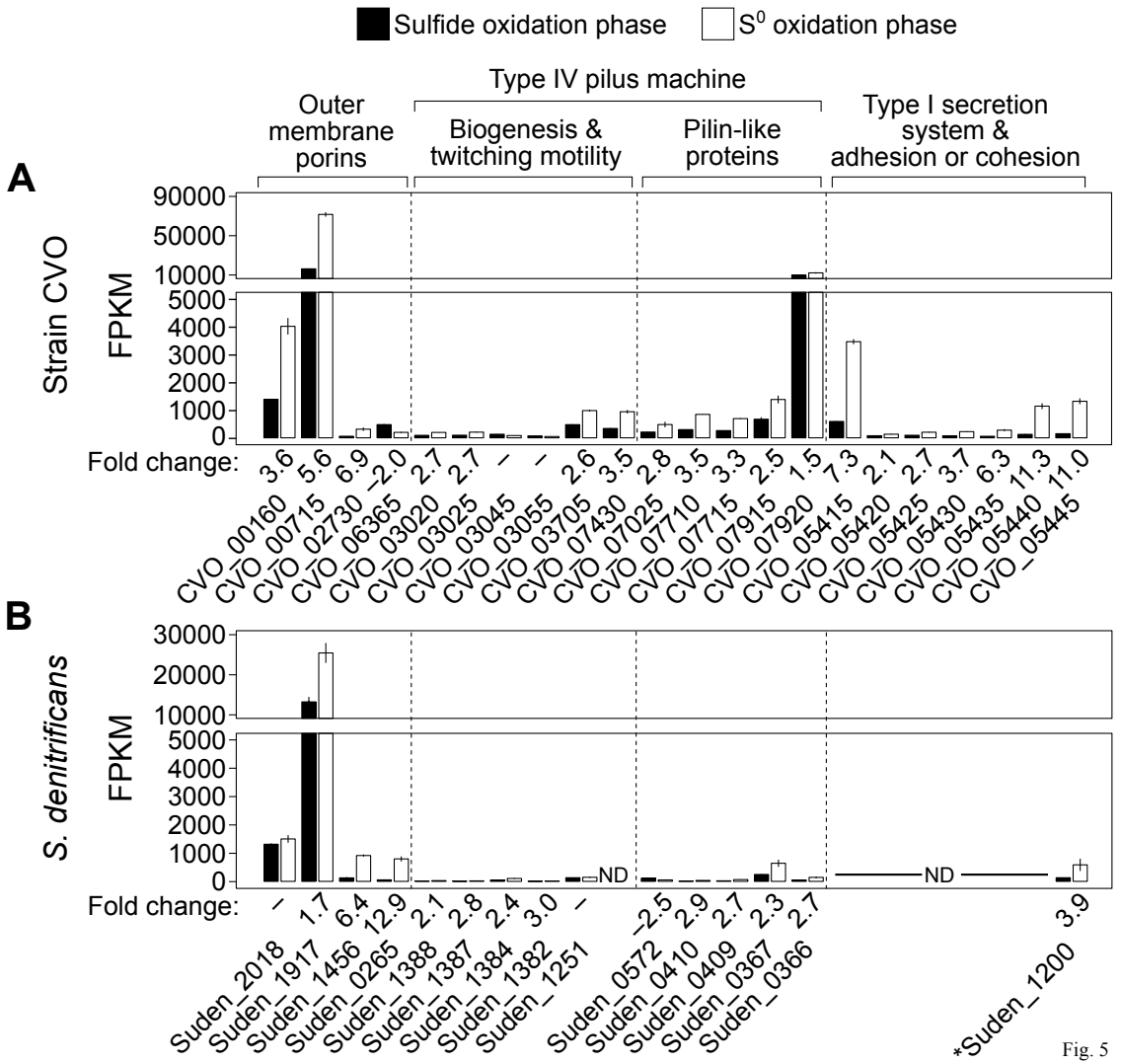
Sulfide oxidation phase
S0 oxidation phase
Type IV pilus machine
Outer membrane porins
Biogenesis & twitching motility
Pilin-like proteins
Type I secretion system & adhesion or cohesion
A
Strain CVO
FPKM
90000
50000
10000
5000
4000
3000
2000
1000
0
Fold change:
3.6 5.6 6.9 −2.0 2.7 2.7 − − 2.6 3.5 2.8 3.5 3.3 2.5 1.5 7.3 2.1 2.7 3.7 6.3 11.3 11.0
CVO_00160 CVO_00715 CVO_02730 CVO_06365 CVO_03020 CVO_03025 CVO_03045 CVO_03055 CVO_03705 CVO_07430 CVO_07025 CVO_07710 CVO_07715 CVO_07915 CVO_07920 CVO_05415 CVO_05420 CVO_05425 CVO_05430 CVO_05435 CVO_05440 CVO_05445
B
S. denitrificans
FPKM
30000
20000
10000
5000
4000
3000
2000
1000
0
ND
ND
Fold change:
− 1.7 6.4 12.9 2.1 2.8 2.4 3.0 − −2.5 2.9 2.7 2.3 2.7 3.9
Suden_2018 Suden_1917 Suden_1456 Suden_0265 Suden_1388 Suden_1387 Suden_1384 Suden_1382 Suden_1251 Suden_0572 Suden_0410 Suden_0409 Suden_0367 Suden_0366 *Suden_1200

Fig. 5

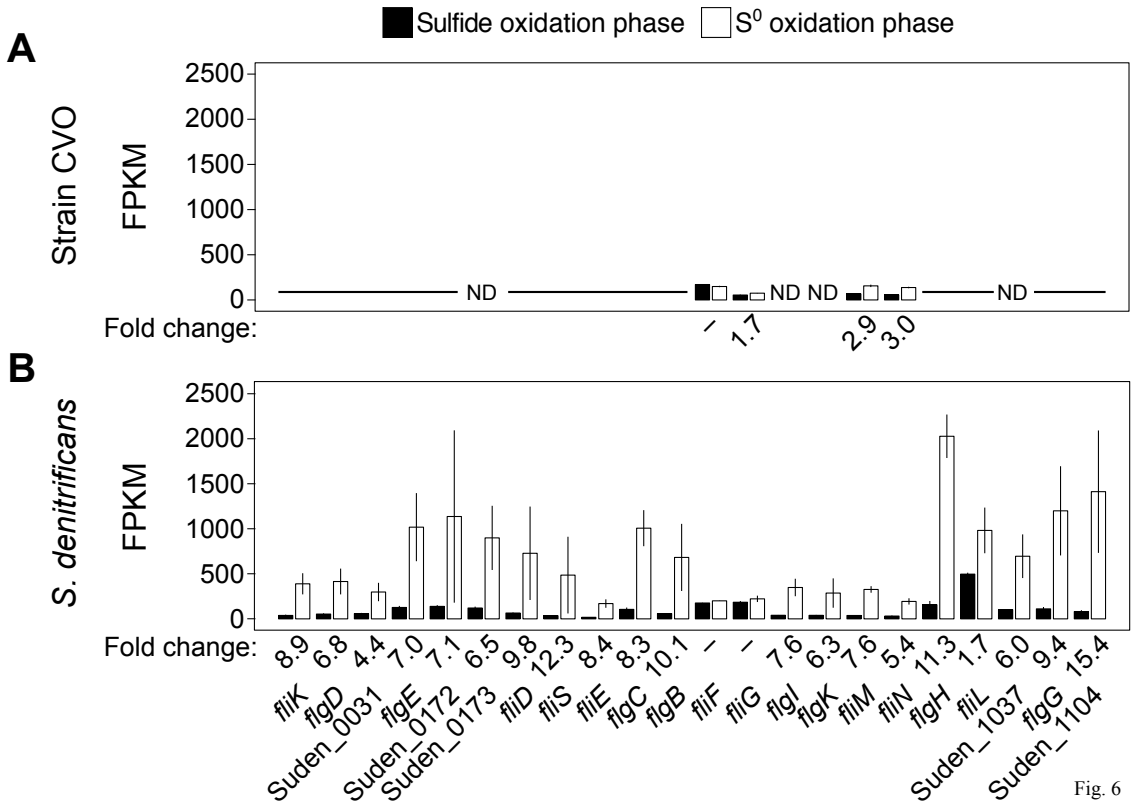
Sulfide oxidation phase
S0 oxidation phase
A
Strain CVO
FPKM
2500
2000
1500
1000
500
0
ND
ND ND
ND
Fold change:
–
1.7
2.9
3.0
B
S. denitrificans
FPKM
2500
2000
1500
1000
500
0
Fold change:
8.9
6.8
4.4
7.0
7.1
6.5
9.8
12.3
8.4
8.3
10.1
–
–
7.6
6.3
7.6
5.4
11.3
1.7
6.0
9.4
15.4
fliK
flgD
Suden_0031
flgE
Suden_0172
Suden_0173
fliD
fliS
fliE
flgC
flgB
fliF
fliG
flgI
flgK
fliM
fliN
flgH
fliL
Suden_1037
flgG
Suden_1104

Fig. 6

Supplementary Methods:

Strains and growth conditions

Sulfurimonas sp. strain CVO (NRRL B-21472) was obtained from the Agricultural Research Service Culture Collection Northern Regional Research Laboratory (ARS NRRL, US). *Sulfurimonas denitrificans* DSM 1251 was obtained from the German Collection of Microorganisms and Cell Cultures (DSMZ). Strain purity was verified by microscopy and sequencing of the 16S rRNA gene.

Strains were routinely cultured under anaerobic conditions in modified Coleville synthetic brine medium (CSB-A) as recently described (Hubert et al. 2003; Lahme et al. 2019). The medium contained the following salts (per Liter): 7.0 g NaCl, 0.2 g KH_2PO_4, 0.25 NH_4Cl, 0.15 g $CaCl_2 \cdot 2 H_2O$, 0.4 g $MgCl_2 \cdot 6 H_2O$, 0.5 g KCl. For cultivation of *S. denitrificans* addition of NaCl was omitted as it inhibited growth. After autoclaving and cooling under a N_2/CO_2 (90:10) atmosphere the medium was supplemented with 30 ml $NaHCO_3$ (1 M), vitamins trace elements, selenite and tungstate solution and resazurin as described elsewhere (Widdel and Bak 1992; Hubert et al. 2003). The pH was adjusted to around 7.0, the medium dispensed into serum bottles, headspace exchanged with N_2/CO_2 (90:10) and bottles sealed with butyl rubber stoppers and aluminium crimps.

Biogenic S^0 from strain CVO or *S. denitrificans* was prepared as described before (Lahme et al. 2019). Sodium nitrate (2 M), and sodium sulfide, biogenic S^0 or sodium thiosulfate (both 1 M) were added from anoxic stock solutions by means of N_2-flushed syringes.

Gene expression during sulfur compound oxidation coupled with nitrate reduction was assessed in triplicate cultures of strains CVO (4 mM sulfide, 10 mM nitrate) or *S. denitrificans* (2 mM sulfide or 5 mM thiosulfate, and 10 mM nitrate), respectively. For individual experiments 5% (v/v) of three-day old cultures adapted to the respective substrates for five consecutive transfers served as inocula.

Chemical analysis

Samples were taken from cultures with N_2-flushed syringes and either directly analyzed, frozen at –20° C or treated according to specific methodological requirements before freezing as described recently by Lahme et al. (2019). Dissolved sulfide concentrations were directly determined after filtration (0.2 µm, cellulose-acetate) using the spectrophotometric $CuSO_4$ method (Cord-Ruwisch 1985). Concentrations of nitrate, nitrite and sulfate were determined by ion chromatography, and biogenic S^0 was measured by liquid chromatography after extraction with chloroform as described elsewhere (Lahme et al. 2019). Thiosulfate and sulfite were quantified by liquid chromatography after derivatization with monobromobimane as described elsewhere (Callbeck et al. 2018; Lahme et al. 2019).

Scanning electron microscopy

For scanning electron microscopy *Sulfurimonas* sp. strain CVO or *S. denitrificans* were grown with 15 mM nitrate and either 30 mM chemically produced elemental S^0 (Sigma-Aldrich Merck, UK) or 30 mM biogenic S^0 prepared as described previously (Lahme et al. 2019). After 10 days S^0 particles were harvested by brief centrifugation (2 min, 9000 g) and cells fixed by incubating the S^0 in 2% glutaraldehyde in Sorensen's phosphate buffer (0.133 M Na_2HPO_4/KH_2PO_4, pH 7.2) overnight at room temperature. Afterwards the samples were again briefly centrifuged and dehydrated by consecutive 30 min incubations in 25%, 50%, 75% ethanol in phosphate buffer and 60 min in 100% ethanol.

A small amount of S^0 particles were air dried on sticky carbon discs in a desiccator and gold coated prior to analysis at the Electron Microscopy Research Service (Newcastle University, UK). Images were recorded using a Vega 3LMU scanning electron microscope (Tescan, UK).

DNA extraction

Cells of strain CVO were harvested from 200 ml freshly grown culture grown with 4 mM sulfide and 10 mM nitrate by centrifugation (10 min at 5,000 g and 4° C) and washed once in 1 ml Tris-EDTA buffer (TE; 100 mM Tris, 1 mM EDTA, pH 8.0). The cell pellet was resuspended in 450 µl TE buffer containing 15 mg/ml lysozyme (Sigma-Aldrich Merck, UK). After addition of 10 µl RNase A (10 µg/µl; Thermo Fisher Scientific, UK) the sample was incubated for 30 min at 37° C and carefully mixed by inverting every 5 min. Afterwards 25 µl Proteinase K (20 mg/ml; Bioline, UK) was added and incubation continued for further 60 min at 56° C. Afterwards 25 µl NaCl (5 M), 100 µl sodium dodecyl sulfate (10% v/v) and 60 µl sodium acetate (3 M) were added followed by a 15 min incubation at 65° C. After adding 600 µl phenol:chloroform:isoamylalcohol (PCI; 25:24:1) the sample was carefully mixed by inversion for 5 min and then centrifuged (5 min at 15,000 g and 4° C). The liquid phase was collected and the PCI procedure repeated. Subsequently, DNA was precipitated by mixing the liquid phase with 0.7 volumes of isopropanol and collected by centrifugation (30 min at 15,000 g and 4° C). The supernatant was carefully discarded and the DNA pellet washed with 500 µl ethanol (70%, v/v). After another centrifugation (15 min at 15,000 g and 4° C) the supernatant was discarded and the DNA pellet was air dried, resuspended in TE buffer (see above) and then frozen in aliquots at –20° C.

DNA concentration, purity and integrity were determined immediately after extraction via the Qubit® DNA HS assay using an Invitrogen Qubit® 3.0 Fluorometer (Thermo Fisher Scientific, UK), NanoDrop® ND-1000 spectrophotometer (Thermo Scientific, UK) and agarose gel electrophoresis.

***De novo* genome sequencing, assembly and annotation**

DNA from strain CVO was sequenced at the Centre for Genomic Research at the University of Liverpool (UK) on a Pacific Bioscience RSII platform using a 10kb library preparation protocol and P6-C4 chemistry. Library was sequenced on a Single Molecule Real-Time (SMRT®) cell. Additional paired-end sequencing (2x 300 bp) was performed at the Centre for Bacterial Cell Biology (Newcastle University) on the Illumina MiSeq platform using Miseq reagent kit v3 and the Nextera XT kit (Illumina, UK) for library preparation, following the manufacturer's instructions.

After removing adapter sequences and quality trimming of raw reads, *de novo* genomes were assembled with the SPAdes Genome Assembler (v 3.6.2) using the hybrid assembly function with automatic *k*-mer size selection and read error correction enabled (Bankevich et al. 2012). The assembly resulted in a single high coverage scaffold, which was subsequently manually closed by merging overlapping ends in Artemis (Rutherford et al. 2000). Structural and functional annotation was performed using the National Center for Biotechnology Information (NCBI) prokaryotic annotation pipeline (Tatusova et al. 2016; Haft et al. 2018). Functional predictions and annotations of selected genes, referred to in this study, were manually inspected by comparing the automatic annotation to hidden Markov model-based (Eddy 2011) searches using InterPro (Mitchell et al. 2019), as well as BLASTP comparison against the NCBI non-redundant protein sequence database (Camacho et al. 2009) or the curated UniProtKB/Swiss-Prot protein sequence database (Boutet et al. 2007).

The sequencing reads used for *de novo* genome reconstruction have been deposited at the NCBI Sequence Read Archive (SRA) under the accession number PRJNA482764.The annotated genome from strain CVO has been deposited at GenBank under accession number CP033720.

RNA sampling and extraction

For extraction of RNA, cells from triplicate cultures for each strain were harvested during active oxidation of sulfide or biogenic zero-valent sulfur, as well as thiosulfate in case of *S. denitrificans* (see Fig. 1 and Fig. S1). Samples were removed using N_2-flushed syringes and RNA was preserved by immediate mixing with RNAprotect® Bacterial Reagent (Qiagen) according to the manufacturer's instructions. Cells were harvested by centrifugation (5,000 g, 10 min), the supernatant discarded and the cell pellet frozen at –80° C. RNA was extracted from frozen pellets within four weeks of cell harvesting. Cell pellets were thawed on ice, resuspended in 100 µl TE buffer containing 15 mg/ml lysozyme (see DNA extraction for details) and incubated for 10 min at room temperature. Further extraction of RNA was performed with the Isolate II RNA mini kit (Bioline, UK) including an on-column DNase I digestion step. After elution in RNase-free water RNA was subjected to another DNA digestion with RNase-free DNase I (Thermo Fisher Scientific, UK) in the presence of RiboLock™ RNase inhibitor (Thermo Fisher Scientific, UK). The RNA was cleaned and concentrated using Zyme Research RNA Clean and Concentrator-5 (Cambridge Biosciences Ltd., UK). RNA was eluted in RNase-free water, aliquoted and stored at –80° C. RNA integrity was controlled by the RNA 6000 Nano assay using the Agilent 2100 Bioanalyzer (Agilent Technologies, UK). RNA purity was assessed with a NanoDrop® ND-1000 spectrophotometer (Thermo Scientific, UK) and RNA concentration was additionally confirmed with the Qubit® RNA HS Assay using an Invitrogen Qubit® 3.0 Fluorometer (Thermo Fisher Scientific, UK). Removal of DNA was verified by PCR using the universal 16S rRNA gene primer pairs targeting the V4-V5 region (Caporaso et al. 2012).

RNA sequencing and differential gene expression analysis

For preparation of RNA sequencing libraries, rRNA was first removed using the Ribo-Zero rRNA Removal Kit for bacteria (Illumina, UK). Subsequently, RNA sequencing libraries were prepared using the ScripSeq v2 kit according to manufacturer's instructions. Paired-end sequencing (2x 125bp) of multiplexed libraries was performed on an Illumina HiSeq 2500 with SBS V4 chemistry. Raw sequencing reads obtained from strain CVO and *S. denitrificans* transcriptomes have been deposited at NCBI's SRA under the accession numbers PRJNA482764 and PRJNA504592, respectively.

Analysis of differentially expressed genes was conducted using CLC Genomic Workbench (v. 10.1.1; Qiagen, UK). After demultiplexing and adapter removal, reads were uploaded into CLC Genomic Workbench and quality trimmed. 10 million paired-end reads were subsampled from each replicate library and mapped to the reference genomes with the following alignment parameters: mismatch cost = 2, insertion cost = 3, deletion cost = 3, length fraction = 0.8, similarity fraction = 0.8. For quantification of gene expression, reads mapped to individual genes were counted and normalized for gene length and total library size to generate normalized FPKM (fragments mapped per kilobase per million reads) expression values (Mortazavi et al. 2008). In this regard, paired-end reads mapped to the same gene were counted as one rather than two mapped reads.

For *S. denitrificans* and CVO an empirical differential gene expression (DGE) analysis was conducted in CLC Genomic Workbench, which implements the 'Exact Test' to estimate negative binomial dispersion as previously described (Robinson and Smyth 2008). The DGE analysis either

compared gene expression during sulfide oxidation with gene expression during biogenic S^0 oxidation phase (for both strains), or with active thiosulfate oxidation (only for *S. denitrificans*). DGE significance was assessed using the CLC implemented Gaussian-based *t*-test to perform a two-group comparison, with false discovery rate (FDR) correction applied to the original *p*-values based on the method described by Benjamini and Hochberg (1995). FDR corrected *p*-values <0.01 were used as a threshold for significant differential expression.

Nucleotide and protein sequence analysis

Nucleotide and amino acid sequences were retrieved from Genbank and the Integrated Microbial Genomes and Metagenomes (IMG/M) databases (Clark et al. 2016; Chen et al. 2017). Amino acid sequences of sulfide quinone oxidoreductases were aligned with the MUSCLE program (Edgar 2004). Phylogenetic trees were constructed with the Maximum-Likelihood method with 500 bootstrap iterations in MEGA7 (Kumar et al. 2016). Structural and topological predictions of outer membrane proteins were performed with amino acid sequences via the web-based software BOCTOPUS2, PRED-TMBB2 and Phyre2 (Kelley et al. 2015; Hayat et al. 2016; Tsirigos et al. 2016).

References:

Bankevich A, Nurk S, Antipov D, et al (2012) SPAdes: A New Genome Assembly Algorithm and Its Applications to Single-Cell Sequencing. J Comput Biol 19:455–477. doi: 10.1089/cmb.2012.0021

Benjamini Y, Hochberg Y (1995) Controlling the False Discovery Rate: A Practical and Powerful Approach to Multiple Testing. J R Stat Soc Ser B Methodol 57:289–300

Boutet E, Lieberherr D, Tognolli M, et al (2007) UniProtKB/Swiss-Prot. Methods Mol Biol Clifton NJ 406:89–112

Camacho C, Coulouris G, Avagyan V, et al (2009) BLAST+: architecture and applications. BMC Bioinformatics 10:421. doi: 10.1186/1471-2105-10-421

Caporaso JG, Lauber CL, Walters WA, et al (2012) Ultra-high-throughput microbial community analysis on the Illumina HiSeq and MiSeq platforms. ISME J 6:1621–1624. doi: 10.1038/ismej.2012.8

Chen I-MA, Markowitz VM, Chu K, et al (2017) IMG/M: integrated genome and metagenome comparative data analysis system. Nucleic Acids Res 45:D507–D516. doi: 10.1093/nar/gkw929

Clark K, Karsch-Mizrachi I, Lipman DJ, et al (2016) GenBank. Nucleic Acids Res 44:D67–D72. doi: 10.1093/nar/gkv1276

Eddy SR (2011) Accelerated Profile HMM Searches. PLOS Comput Biol 7:e1002195. doi: 10.1371/journal.pcbi.1002195

Edgar RC (2004) MUSCLE: multiple sequence alignment with high accuracy and high throughput. Nucleic Acids Res 32:1792–1797. doi: 10.1093/nar/gkh340

Haft DH, DiCuccio M, Badretdin A, et al (2018) RefSeq: an update on prokaryotic genome annotation and curation. Nucleic Acids Res 46:D851–D860. doi: 10.1093/nar/gkx1068

Hayat S, Peters C, Shu N, et al (2016) Inclusion of dyad-repeat pattern improves topology prediction of transmembrane β-barrel proteins. Bioinforma Oxf Engl 32:1571–1573. doi: 10.1093/bioinformatics/btw025

Kelley LA, Mezulis S, Yates CM, et al (2015) The Phyre2 web portal for protein modelling, prediction and analysis. Nat Protoc 10:845–858. doi: 10.1038/nprot.2015.053

Kumar S, Stecher G, Tamura K (2016) MEGA7: Molecular Evolutionary Genetics Analysis Version 7.0 for Bigger Datasets. Mol Biol Evol 33:1870–1874. doi: 10.1093/molbev/msw054

Lahme S, Enning D, Callbeck CM, et al (2019) Metabolites of an Oil Field Sulfide-Oxidizing, Nitrate-Reducing Sulfurimonas sp. Cause Severe Corrosion. Appl Env Microbiol 85:e01891-18. doi: 10.1128/AEM.01891-18

Mitchell AL, Attwood TK, Babbitt PC, et al (2019) InterPro in 2019: improving coverage, classification and access to protein sequence annotations. Nucleic Acids Res 47:D351–D360. doi: 10.1093/nar/gky1100

Mortazavi A, Williams BA, McCue K, et al (2008) Mapping and quantifying mammalian transcriptomes by RNA-Seq. Nat Methods 5:621–628. doi: 10.1038/nmeth.1226

Robinson MD, Smyth GK (2008) Small-sample estimation of negative binomial dispersion, with applications to SAGE data. Biostat Oxf Engl 9:321–332. doi: 10.1093/biostatistics/kxm030

Rutherford K, Parkhill J, Crook J, et al (2000) Artemis: sequence visualization and annotation. Bioinforma Oxf Engl 16:944–945

Tatusova T, DiCuccio M, Badretdin A, et al (2016) NCBI prokaryotic genome annotation pipeline. Nucleic Acids Res 44:6614–6624. doi: 10.1093/nar/gkw569

Tsirigos KD, Elofsson A, Bagos PG (2016) PRED-TMBB2: improved topology prediction and detection of beta-barrel outer membrane proteins. Bioinforma Oxf Engl 32:i665–i671. doi: 10.1093/bioinformatics/btw444

Table S1 Summary of differential gene expression parameters for cultures of *Sulfurimonas* sp. CVO and *Sulfurimonas denitrificans*.

Locus tag	Gene	Putative function	Gene expression value						Differential expression (S^0 *vs.* H_2S)		Differential expression ($S_2O_3^{2-}$ *vs.* S^0)	
			Sulfide oxidation (H_2S)		Sulfur oxidation (S^0)		Thiosulfate oxidation					
			Mean FPKM	Standard deviation	Mean FPKM	Standard deviation	Mean FPKM	Standard deviation	Fold change	FDR corrected *p*-value	Fold change	FDR corrected *p*-value
***Sulfurimonas* sp. strain CVO:**												
CVO_09655	*sqrB*	Type II sulfide quinone oxidoreductase	1917	145	15477	805	NA	NA	10.0	0.00	NA	NA
CVO_06770	*sqrD*	Type IV sulfide quinone oxidoreductase	256	19	18246	544	NA	NA	88.2	0.00	NA	NA
CVO_05505	*sqrF*	Type VI sulfide quinone oxidoreductase	160	12	59	5	NA	NA	-2.2	0.00	NA	NA
CVO_09755	*soxC*	Sulfur-oxidation protein, sulfur dehydrogenase SoxC	157	8	5949	590	NA	NA	46.9	0.00	NA	NA
CVO_09760	*soxD*	Sulfur-oxidation protein, cytochrome c subunit SoxD	133	16	5286	463	NA	NA	49.2	0.00	NA	NA
CVO_09765	*soxY*	Sulfur-oxidation protein, sulfur carrier subunit SoxY	119	27	4363	250	NA	NA	45.4	0.00	NA	NA
CVO_09770	*soxZ*	Sulfur-oxidation protein, sulfur carrier subunit SoxZ	156	4	4661	355	NA	NA	36.9	0.00	NA	NA
CVO_09775	*soxH*	Metallo hydrolase	94	5	2328	125	NA	NA	30.7	0.00	NA	NA
CVO_07270	*psrA1*	Polysulfide reductase, molydopterin dinucleotide binding subunit A	99	2	899	65	NA	NA	11.2	0.00	NA	NA
CVO_07275	*psrC1*	Polysulfide reductase, membrane subunit C	65	5	594	77	NA	NA	11.3	0.00	NA	NA
CVO_07280	*psrB1*	Polysulfide-reductase, Fe-S-cluster-containing subunit B	74	2	589	84	NA	NA	9.9	0.00	NA	NA
CVO_09630	*psrC2*	Polysulfide reductase, membrane subunit C	1563	53	334	34	NA	NA	-3.8	0.00	NA	NA
CVO_09635	*psrB2*	Polysulfide-reductase, Fe-S-cluster-containing subunit B	2240	55	466	30	NA	NA	-3.9	0.00	NA	NA
CVO_09640	*psrA2*	Polysulfide reductase, molydopterin dinucleotide binding subunit A	3138	33	635	48	NA	NA	-4.0	0.00	NA	NA
CVO_00160		OmpA-like outer membrane protein	1390	21	4024	298	NA	NA	3.6	0.00	NA	NA
CVO_00715		OprD-like outer membrane protein	15989	465	71710	2311	NA	NA	5.6	0.00	NA	NA
CVO_02730		OprD-like outer membrane protein	56	2	311	63	NA	NA	6.9	0.00	NA	NA
CVO_06365		OprD-like outer membrane protein	476	23	196	20	NA	NA	-2.0	0.00	NA	NA
CVO_03020		Type IV general secretion pathway protein, PilC-like	89	3	194	6	NA	NA	2.7	0.00	NA	NA
CVO_03025		Type IV general secretion pathway protein, PilB-like	94	5	204	16	NA	NA	2.7	0.00	NA	NA
CVO_03045		Type IV general secretion pathway protein, PilQ-like	129	8	82	3	NA	NA	-1.3	0.00	NA	NA
CVO_03055		Type IV Pilus assembly protein, PilO-like	69	7	47	4	NA	NA	-1.2	0.01	NA	NA
CVO_03705		Type IV pilus twitching motility protein PilT-like	475	17	982	32	NA	NA	2.6	0.00	NA	NA
CVO_07430		Type IV pilus twitching motility protein PilT-like	337	19	941	64	NA	NA	3.5	0.00	NA	NA
CVO_07025		putative pilin precursor	208	16	479	100	NA	NA	2.8	0.00	NA	NA
CVO_07710		putative pilin precursor	295	9	845	3	NA	NA	3.5	0.00	NA	NA
CVO_07715		putative pilin precursor	260	2	693	14	NA	NA	3.3	0.00	NA	NA
CVO_07915		putative pilin precursor	672	73	1383	140	NA	NA	2.5	0.00	NA	NA
CVO_07920		putative pilin precursor	9583	455	11833	722	NA	NA	1.5	0.00	NA	NA
CVO_05415		type I secretion outer membrane protein, TolC family	590	11	3469	92	NA	NA	7.3	0.00	NA	NA
CVO_05420		ATP-binding cassette	75	2	129	10	NA	NA	2.1	0.00	NA	NA
CVO_05425		Membrane fusion protein	92	2	202	13	NA	NA	2.7	0.00	NA	NA
CVO_05430		DNA-binding response regulator	74	6	222	15	NA	NA	3.7	0.00	NA	NA
CVO_05435		Cadherin domain-containing protein	54	3	277	36	NA	NA	6.3	0.00	NA	NA
CVO_05440		hypothetical protein	125	15	1143	106	NA	NA	11.3	0.00	NA	NA
CVO_05445		VCBS repeat and cadherin-domain containing RTX family protein	148	15	1319	105	NA	NA	11.0	0.00	NA	NA
CVO_07390	*fliF*	flagellar basal-body M-ring protein FliF	171	5	149	7	NA	NA	1.1	0.15	NA	NA
CVO_07385	*fliG*	flagellar motor switch protein FliG	54	5	75	2	NA	NA	1.7	0.00	NA	NA
CVO_06455	*fliM*	flagellar motor switch protein FliM	67	4	156	13	NA	NA	2.9	0.00	NA	NA
CVO_06450	*fliN*	flagellar motor switch protein FliN	56	8	137	8	NA	NA	3.0	0.00	NA	NA
***Sulfurimonas denitrificans* DSM 1251:**												
Suden_2082	*sqrB*	Type II sulfide quinone oxidoreductase	3373	41	9924	1372	7567	295	2.5	0.00	-1.4	0.00
Suden_1879	*sqrC*	Type III sulfide quinone oxidoreductase	18	2	669	251	19	2	32.8	0.00	-38.6	0.00
Suden_0619	*sqrD*	Type IV sulfide quinone oxidoreductase	881	169	5337	750	5585	165	5.2	0.00	-1.0	0.87
Suden_0260	*soxX*	Sulfur-oxidation protein, c-type cytochrome SoxX	41	8	2376	395	3379	39	49.7	0.00	1.3	0.02
Suden_0261	*soxY1*	Sulfur-oxidation protein, sulfur carrier subunit SoxY	17	1	734	186	1247	33	36.9	0.00	1.6	0.00
Suden_0262	*soxZ1*	Sulfur-oxidation protein, sulfur carrier subunit SoxZ	62	3	2653	562	5098	95	37.3	0.00	1.8	0.00
Suden_0263	*soxA*	Sulfur-oxidation protein, diheme cytochrome SoxA	49	1	1599	258	2779	29	28.0	0.00	1.6	0.00
Suden_0264	*soxB*	Sulfur-oxidation protein, sulfate thiol esterase SoxB	43	3	908	163	2270	46	18.4	0.00	2.4	0.00
Suden_2060	*soxC*	Sulfur-oxidation protein, sulfur dehydrogenase SoxC	2937	127	6434	510	4019	54	1.6	0.00	-2.6	0.00
Suden_2059	*soxD*	Sulfur-oxidation protein, cytochrome c subunit SoxD	8721	478	16222	538	10935	563	1.5	0.00	-2.4	0.00
Suden_2058	*soxY2*	Sulfur-oxidation protein, sulfur carrier subunit SoxY	5193	132	10023	484	6630	396	1.7	0.00	-1.6	0.00
Suden_2057	*soxZ2*	Sulfur-oxidation protein, sulfur carrier subunit SoxZ	5059	542	8664	951	3786	34	1.6	0.00	-1.6	0.00
Suden_2056	*soxH*	Metallo hydrolase	6125	657	11009	1296	4558	159	1.9	0.00	-1.7	0.00
Suden_0500	*psrA*	Polysulfide reductase, molydopterin dinucleotide binding subunit A	1240	78	2095	297	1504	52	1.3	0.01	-1.5	0.00
Suden_0499	*psrC*	Polysulfide reductase, membrane subunit C	1818	104	2817	332	1694	44	1.3	0.04	-1.8	0.00
Suden_0498	*psrB*	Polysulfide-reductase, Fe-S-cluster-containing subunit B	1606	98	2412	31	1708	59	1.5	0.01	-1.5	0.00
Suden_2018		OmpA-like outer membrane protein	1317	33	1504	135	1488	19	-1.0	0.94	-1.1	0.55
Suden_1917		OprD-like outer membrane protein	13142	1258	25422	2499	28501	489	1.7	0.00	1.1	0.54
Suden_1456		OprD-like outer membrane protein	124	31	916	38	195	7	6.4	0.00	-5.0	0.00
Suden_0265		OprD-like outer membrane protein	53	6	796	90	2436	28	12.9	0.00	2.9	0.00
Suden_1388		Type IV general secretion pathway protein, PilC-like	11	1	26	4	32	1	2.1	0.00	1.1	0.35
Suden_1387		Type IV general secretion pathway protein, PilB-like	6	2	18	4	31	1	2.8	0.00	1.7	0.00
Suden_1384		Type IV general secretion pathway protein, PilQ-like	38	5	103	14	110	2	2.4	0.00	1.0	0.98
Suden_1382		Type IV Pilus assembly protein, PilO-like	4	1	15	1	19	1	3.0	0.00	1.2	0.43
Suden_1251		Type IV pilus twitching motility protein PilT-like	129	4	145	22	174	5	-1.0	0.83	1.1	0.43
Suden_0572		putative pilin precursor	108	7	51	8	119	10	-2.5	0.00	2.2	0.00
Suden_0410		putative pilin precursor	10	2	32	5	48	2	2.9	0.00	1.4	0.02
Suden_0409		putative pilin precursor	20	7	63	6	55	4	2.7	0.00	-1.2	0.05
Suden_0367		putative pilin precursor	245	15	642	128	610	34	2.3	0.00	-1.1	0.42
Suden_0366		putative pilin precursor	46	20	141	34	159	14	2.7	0.00	1.1	0.69
Suden_1200		Ca-binding RTX-family protein	129	10	586	217	265	14	3.9	0.00	-2.4	0.00
Suden_0029	*fliK*	Flagellar hook-length control protein FliK	38	9	388	117	79	0	8.9	0.00	-5.3	0.00
Suden_0030	*flgD*	Flagellar hook assembly protein FlgD	53	9	413	143	110	4	6.8	0.00	-4.0	0.00
Suden_0031		flagellar hook-basal body protein	58	8	297	102	93	2	4.4	0.00	-3.4	0.00
Suden_0032	*flgE*	flagellar hook protein FlgE, epsilon proteobacterial	126	17	1014	377	278	7	7.0	0.00	-3.9	0.00
Suden_0172		Flagellin and related hook-associated protein FlgL	138	14	1132	953	258	4	7.1	0.00	-4.7	0.00
Suden_0173		Flagellin and related hook-associated protein FlgL	120	15	896	355	301	8	6.5	0.00	-3.2	0.00
Suden_0202	*fliD*	Flagellar capping protein FliD	65	6	725	517	116	4	9.8	0.00	-6.7	0.00
Suden_0203	*fliS*	flagellar biosynthetic protein FliS	34	1	484	424	51	3	12.3	0.00	-10.1	0.00
Suden_0363	*fliE*	flagellar hook-basal body complex protein FliE	17	2	169	47	56	2	8.4	0.00	-3.3	0.00
Suden_0364	*flgC*	flagellar basal-body rod protein FlgC	105	20	1003	199	231	7	8.3	0.00	-4.7	0.00
Suden_0365	*flgB*	flagellar basal-body rod protein FlgB	59	3	680	371	142	8	10.1	0.00	-5.2	0.00
Suden_0472	*fliF*	Flagellar FliF M-ring protein	175	3	200	2	271	5	-1.02	0.90	1.3	0.08
Suden_0473	*fliG*	Flagellar motor switch protein FliG	184	13	221	35	259	10	1.0	0.78	1.1	0.43
Suden_0562	*flgI*	Flagellar basal body P-ring protein FlgI	40	3	347	97	76	3	7.6	0.00	-4.9	0.00
Suden_0566	*flgK*	flagellar hook-associated protein FlgK	39	5	285	162	75	2	6.3	0.00	-4.1	0.00
Suden_0707	*fliM*	flagellar motor switch protein FliM	37	4	325	36	75	6	7.6	0.00	-4.6	0.00
Suden_0708	*fliN*	flagellar motor switch protein FliN	31	6	193	35	78	4	5.4	0.00	-2.7	0.00
Suden_0733	*flgH*	Flagellar basal body L-ring protein FlgH	156	42	2020	241	384	12	11.3	0.00	-5.6	0.00
Suden_0840	*fliL*	Flagellar basal body associated protein	495	16	978	253	656	5	1.7	0.00	-1.6	0.00
Suden_1037		Flagellin and related hook-associated protein FlgL	101	2	693	241	155	3	6.0	0.00	-4.8	0.00
Suden_1103	*flgG*	flagellar basal-body rod protein FlgG, Gram-negative bacteria	111	21	1195	493	244	6	9.4	0.00	-5.2	0.00
Suden_1104		flagellar hook-basal body protein	80	16	1407	677	175	7	15.4	0.00	-8.7	0.00

NA = Not applicable; * amino acid sequence contains signal peptide; FPKM: Fragments per kilobase and million reads; FDR: False discovery rate

Table S2 Information of metagenome-assembled genomes (MAG) of *Sulfurimonas* spp. from different habitats shown in Figure 4 of the main manuscript.

Organism	Source	Biosample	Accession	Completeness CheckM (%)	Reference*
Sulfurimonas sp. GWF2_37_8	Subsurface aquifer (Rifle, Colorado, USA)	SAMN04314140	MIBW00000000.1	84.9	Anantharaman *et al*., 2016
Sulfurimonas sp. RIFCSPHIGHO2_12_FULL_36_9	Subsurface aquifer (Rifle, Colorado, USA)	SAMN04315574	MIBX00000000.1	83.3	Anantharaman *et al*., 2016
Sulfurimonas sp. RIFCSPLOWO2_02_FULL_36_28	Subsurface aquifer (Rifle, Colorado, USA)	SAMN04316114	MIBY00000000.1	78.0	Anantharaman *et al*., 2016
Sulfurimonas sp. RIFCSPLOWO2_12_36_12	Subsurface aquifer (Rifle, Colorado, USA)	SAMN04313803	MIBZ00000000.1	98.4	Anantharaman *et al*., 2016
Sulfurimonas sp. RIFCSPLOWO2_12_FULL_34_6	Subsurface aquifer (Rifle, Colorado, USA)	SAMN04315862	MICA00000000.1	86.1	Anantharaman *et al*., 2016
Sulfurimonas sp. RIFCSPLOWO2 12 FULL 36 74	Subsurface aquifer (Rifle, Colorado, USA)	SAMN04316202	MICB00000000.1	90.8	Anantharaman *et al*., 2016
Sulfurimonas sp. RIFOXYB12_FULL_35_9	Subsurface aquifer (Rifle, Colorado, USA)	SAMN04314466	MICC00000000.1	97.2	Anantharaman *et al*., 2016
Sulfurimonas sp. RIFOXYB2_FULL_37_5	Subsurface aquifer (Rifle, Colorado, USA)	SAMN04314450	MICD00000000.1	59.2	Anantharaman *et al*., 2016
Sulfurimonas sp. RIFOXYC2_FULL_36_7	Subsurface aquifer (Rifle, Colorado, USA)	SAMN04316184	MICE00000000.1	68.3	Anantharaman *et al*., 2016
Sulfurimonas sp. RIFOXYD12_FULL_33_39	Subsurface aquifer (Rifle, Colorado, USA)	SAMN04314634	MICF00000000.1	99.6	Anantharaman *et al*., 2016
Sulfurimonas sp. RIFOXYD12 FULL 36 11	Subsurface aquifer (Rifle, Colorado, USA)	SAMN04314646	MICG00000000.1	74.1	Anantharaman *et al*., 2016
Sulfurimonas sp. RIFOXYD2_FULL_34_21	Subsurface aquifer (Rifle, Colorado, USA)	SAMN04314651	MICH00000000.1	99.6	Anantharaman *et al*., 2016
Sulfurimonas sp. RIFOXYD2_FULL_37_8	Subsurface aquifer (Rifle, Colorado, USA)	SAMN04314661	MICI00000000.1	79.0	Anantharaman *et al*., 2016
Sulfurimonas sp. UBA10385	Subsurface sediment (Rifle, Colorado, USA)	SAMN07280039	DLUC00000000	85.3	Waite *et al.,* 2017
Sulfurimonas sp. UBA12504	Subsurface aquifer (Rifle, Colorado, USA)	SAMN07280045	DLUD00000000	91.0	Waite *et al.,* 2017
Sulfurimonas sp. CG_4_10_14_0_2_um_filter_36_1607	Groundwater aquifer (Crystal Geyser, Utah, USA)	SAMN06659771	PFNW00000000.1	100.0	Probst *et al.,* 2018
Sulfurimonas sp. CG_4_10_14_3_um_filter_36_910	Groundwater aquifer (Crystal Geyser, Utah, USA)	SAMN06659894	PFJD00000000	100.0	Probst *et al.,* 2018
Sulfurimonas sp. CG_4_8_14_3_um_filter_36_16	Groundwater aquifer (Crystal Geyser, Utah, USA)	SAMN06659961	PFQO00000000	100.0	Probst *et al.,* 2018
Sulfurimonas sp. CG_4_9_14_0_2_um_filter_36_407	Groundwater aquifer (Crystal Geyser, Utah, USA)	SAMN06660005	PFSG00000000	100.0	Probst *et al.,* 2018
Sulfurimonas sp. CG_4_9_14_0_8_um_filter_36_384	Groundwater aquifer (Crystal Geyser, Utah, USA)	SAMN06660034	PFTJ00000000	100.0	Probst *et al.,* 2018
Sulfurimonas sp. CG01_land_8_20_14_3_00_36_23	Groundwater aquifer (Crystal Geyser, Utah, USA)	SAMN06659162	PETN00000000	100.0	Probst *et al.,* 2018
Sulfurimonas sp. CG02_land_8_20_14_3_00_36_67	Groundwater aquifer (Crystal Geyser, Utah, USA)	SAMN06659181	PEUG00000000	100.0	Probst *et al.,* 2018
Sulfurimonas sp. CG03_land_8_20_14_0_80_36_25	Groundwater aquifer (Crystal Geyser, Utah, USA)	SAMN06659205	PEVE00000000	100.0	Probst *et al.,* 2018
Sulfurimonas sp. CG07_land_8_20_14_0_80_36_56	Groundwater aquifer (Crystal Geyser, Utah, USA)	SAMN06659254	PEXB00000000	100.0	Probst *et al.,* 2018
Sulfurimonas sp. CG08_land_8_20_14_0_20_36_33	Groundwater aquifer (Crystal Geyser, Utah, USA)	SAMN06659295	PEYQ00000000	100.0	Probst *et al.,* 2018
Sulfurimonas sp. CG10_big_fil_rev_8_21_14_0_10_36_24	Groundwater aquifer (Crystal Geyser, Utah, USA)	SAMN06659448	PFEO00000000	100.0	Probst *et al.,* 2018
Sulfurimonas sp. CG12_big_fil_rev_8_21_14_0_65_36_1453	Groundwater aquifer (Crystal Geyser, Utah, USA)	SAMN06659566	PFGJ00000000	99.6	Probst *et al.,* 2018
Sulfurimonas sp. CG15_BIG_FIL_POST_REV_8_21_14_020_36_339	Groundwater aquifer (Crystal Geyser, Utah, USA)	SAMN06659580	PFFV00000000	100.0	Probst *et al.,* 2018
Sulfurimonas sp. CG23_combo_of_CG06-09_8_20_14_all_36_33	Groundwater aquifer (Crystal Geyser, Utah, USA)	SAMN06659700	PCRB00000000	100.0	Probst *et al.,* 2018
Sulfurimonas sp. NORP9	Marine subsurface aquifer (Atlantic Ocean, North Pond)	SAMN07568823	NVXO00000000.1	98.8	Tully *et al.,* 2018
Sulfurimonas sp. NORP87	Marine subsurface aquifer (Atlantic Ocean, North Pond)	SAMN07568901	NVUO00000000.1	84.9	Tully *et al.,* 2018
Sulfurimonas sp. NORP168	Marine subsurface aquifer (Atlantic Ocean, North Pond)	SAMN07568982	NVRL00000000.1	58.3	Tully *et al.,* 2018
Sulfurimonas sp. NORP195	Marine subsurface aquifer (Atlantic Ocean, North Pond)	SAMN07569009	NVQK00000000.1	50.0	Tully *et al.,* 2018
Sulfurimonas sp. BM702	Estuary sediment (Berkley, California, USA)	SAMN07982698	PKUL00000000.1	97.1	Barnum *et al.* , unpublished
Sulfurimonas sp. BM502	Estuary sediment (Berkley, California, USA)	SAMN07982697	PPDH00000000.1	95.0	Barnum *et al.* , unpublished

* Anantharaman, K., Brown, C.T., Hug, L.A., Sharon, I., Castelle, C.J., Probst, A.J., et al. (2016) Thousands of Microbial Genomes Shed Light on Interconnected Biogeochemical Processes in an Aquifer System. Nat Commun 7: 13219.

Waite, D.W., Vanwonterghem, I., Rinke, C., Parks, D.H., Zhang, Y., Takai, K., et al. (2017) Comparative Genomic Analysis of the Class Epsilonproteobacteria and Proposed Reclassification to Epsilonbacteraeota (phyl. nov.). Front Microbiol 8

Probst, A.J., Ladd, B., Jarett, J.K., Geller-McGrath, D.E., Sieber, C.M.K., Emerson, J.B., et al. (2018) Differential Depth Distribution of Microbial Function and Putative Symbionts Through Sediment-Hosted Aquifers in the Deep Terrestrial Subsurface. Nat Microbiol 3: 328–336.

Tully, B.J., Wheat, C.G., Glazer, B.T., and Huber, J.A. (2018) A dynamic microbial community with high functional redundancy inhabits the cold, oxic subseafloor aquifer. ISME J 12: 1–16.

Barnum,T.P., Figueroa,I.A., Carlstrom,C.I., Lucas,L.N., Engelbrektson,A.L. and Coates,J.D. (unpublished)

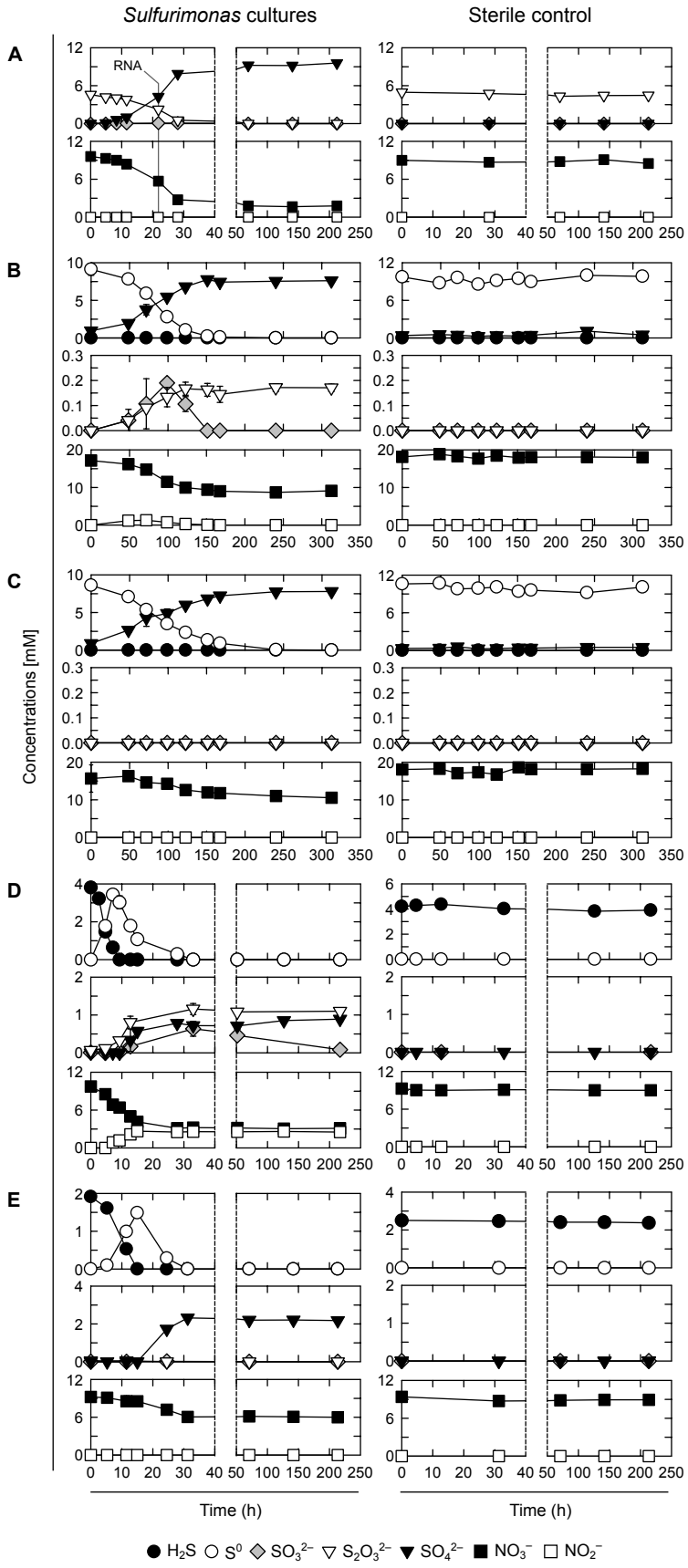

Figure S1 Formation and consumption of sulfur and nitrogen species during nitrate-mediated oxidation of thiosulfate (A), biogenic zero-valent sulfur (B and C) or sulfide (D and E) in *Sulfurimonas* cultures (left panel) and respective sterile controls (right panel). *Sulfurimonas denitrificans* DSM 1251 (A, C and E) and *Sulfurimonas* sp. strain CVO (B and D).

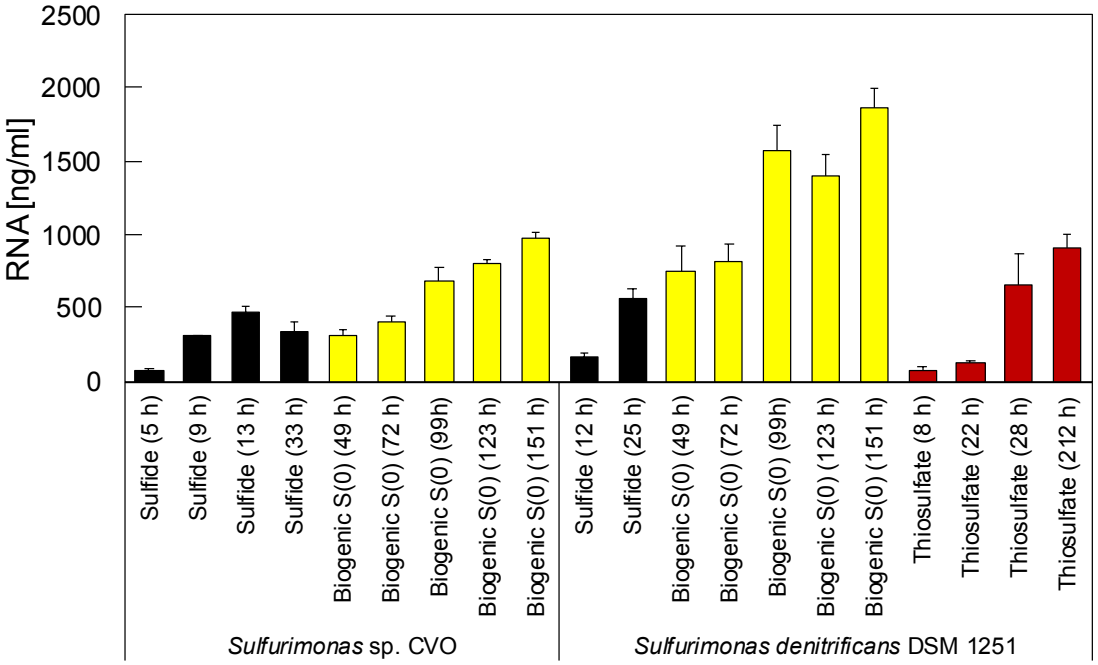

Figure S2 Amount of RNA extracted from cultures of *Sulfurimonas* sp. strain CVO or *Sulfurimonas denitrificans* DSM 1251 when cultivated with different sulfur substrates and nitrate as electron donor and acceptor (see also Fig. 1 and Fig. S1).

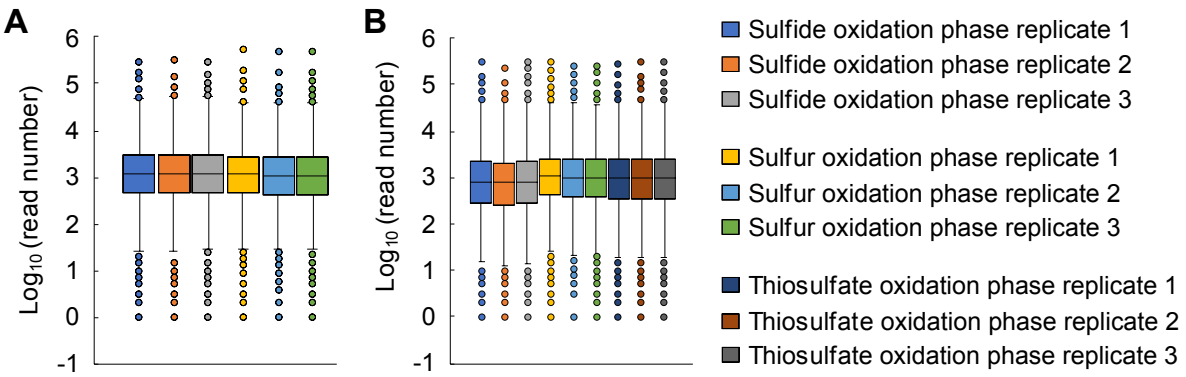

Figure S3 Distribution of raw counts of mapped reads in each replicate across the transcriptomes of A) *Sulfurimonas* sp. strain CVO and B) *Sulfurimonas denitrificans* DSM 1251. The box shows the median of the 1st quartile (lower line) and 3rd quartile (upper line), while the middle line represents the overall median of the data set. The whiskers indicate upper and lower limits of the data and outliers are represented by the filled circles.

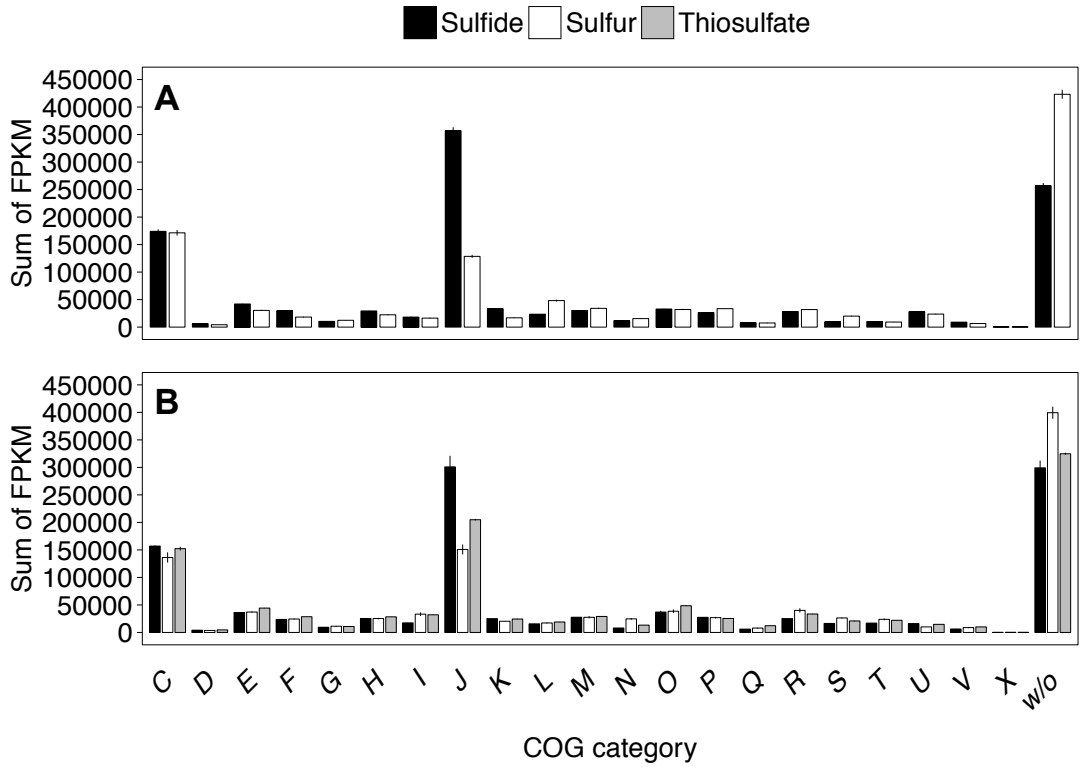

Figure S4 Overall expression of clusters of orthologous genes (COGs) in A) *Sulfurimonas* sp. strain CVO and B) *Sulfurimonas denitrificans* DSM 1251 during sulfide, biogenic zero-valent sulfur (S^0) or thiosulfate oxidation phases. Normalized gene expression is shown as fragments per kilobase and million reads (FPKM). Error bars indicate standard deviation from triplicate cultures.

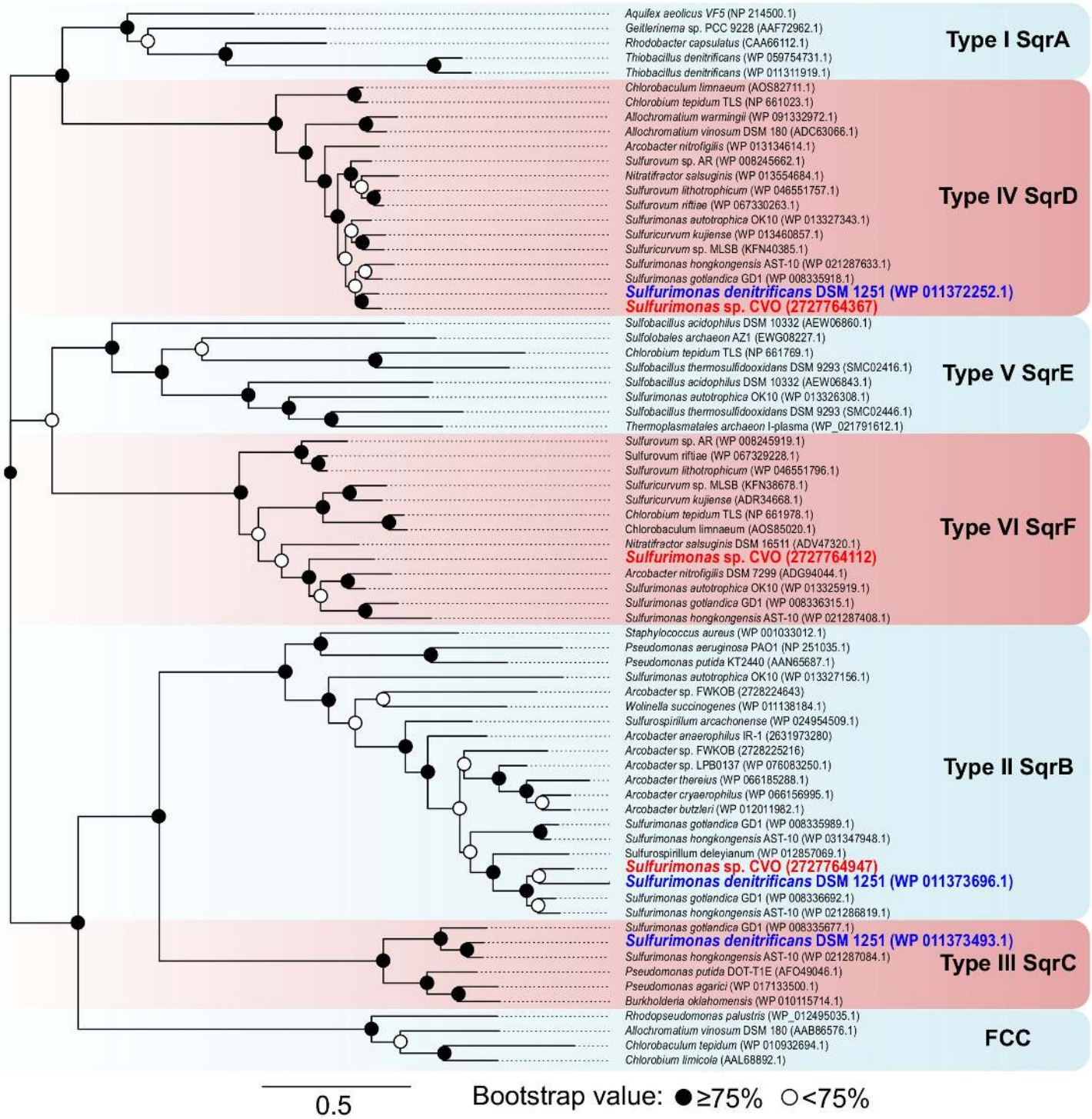

Figure S5 Relationship of sulfide quinone oxidoreductases (SQR) protein sequences from *Sulfurimonas denitrificans* DSM 1251 and *Sulfurimonas* sp. strain CVO with proteins from other bacteria and archaea. Amino acid sequences were derived from the non-redundant protein database at NCBI and accession numbers are shown in brackets. Different SQR subtypes are marked according to previous classifications (Marcia *et al.*, 2010; Gregersen *et al.*, 2011). FCC: Flavocytochrome c sulfide dehydrogenase.

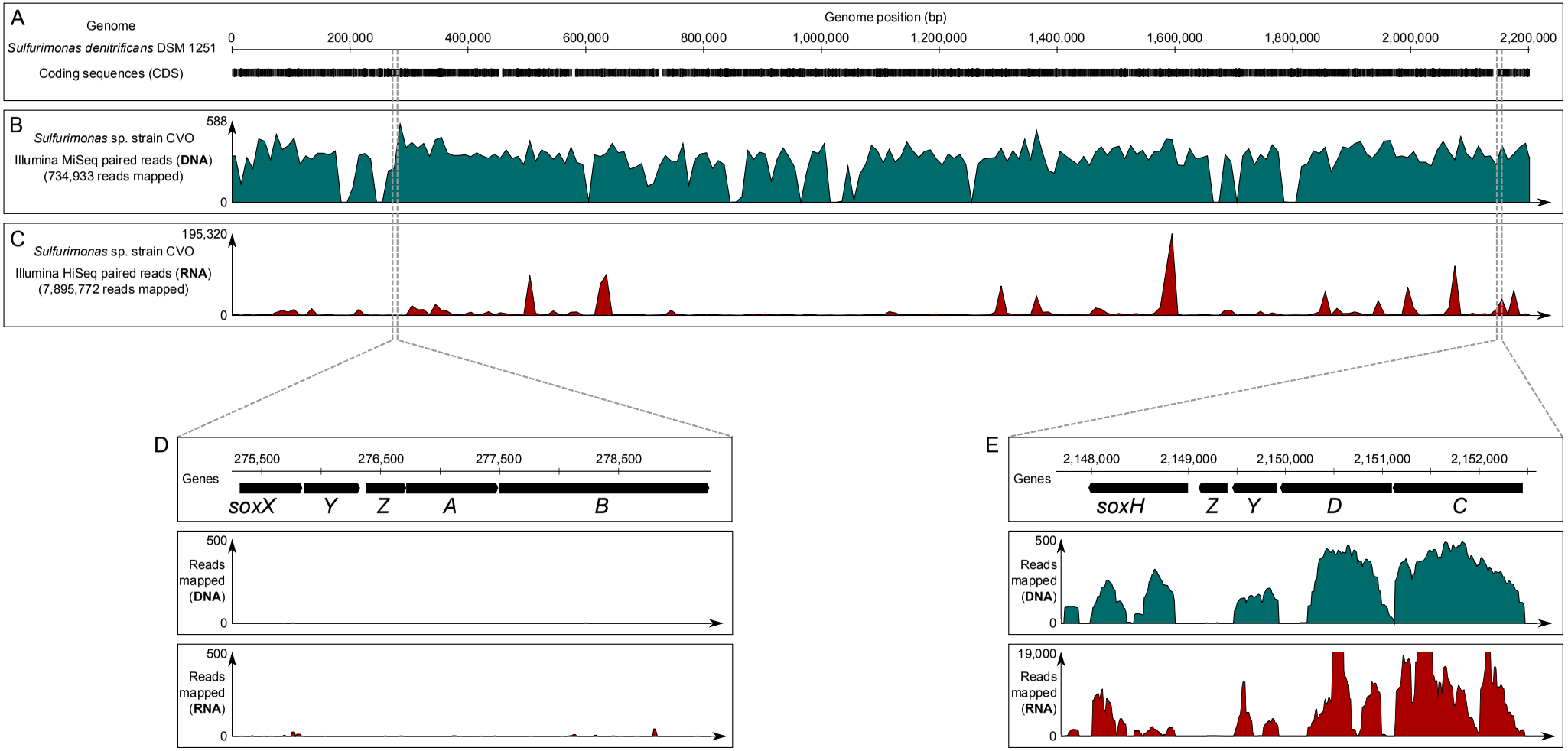

Figure S6 Visualization of cross-mapping reads obtained from sequencing DNA or RNA from strain CVO onto the genome of *Sulfurimonas denitrificans* DSM 1251. A) Genome track with coding sequences marked, B) mapping of Illumina MiSeq reads from DNA of strain CVO C) mapping of Illumina HiSeq reads from RNA of strain CVO. Zoom-in to the D) *soxXY*$_1$*Z*$_1$*AB* genes or E) *soxCDY*$_2$*Z*$_2$*H* genes.

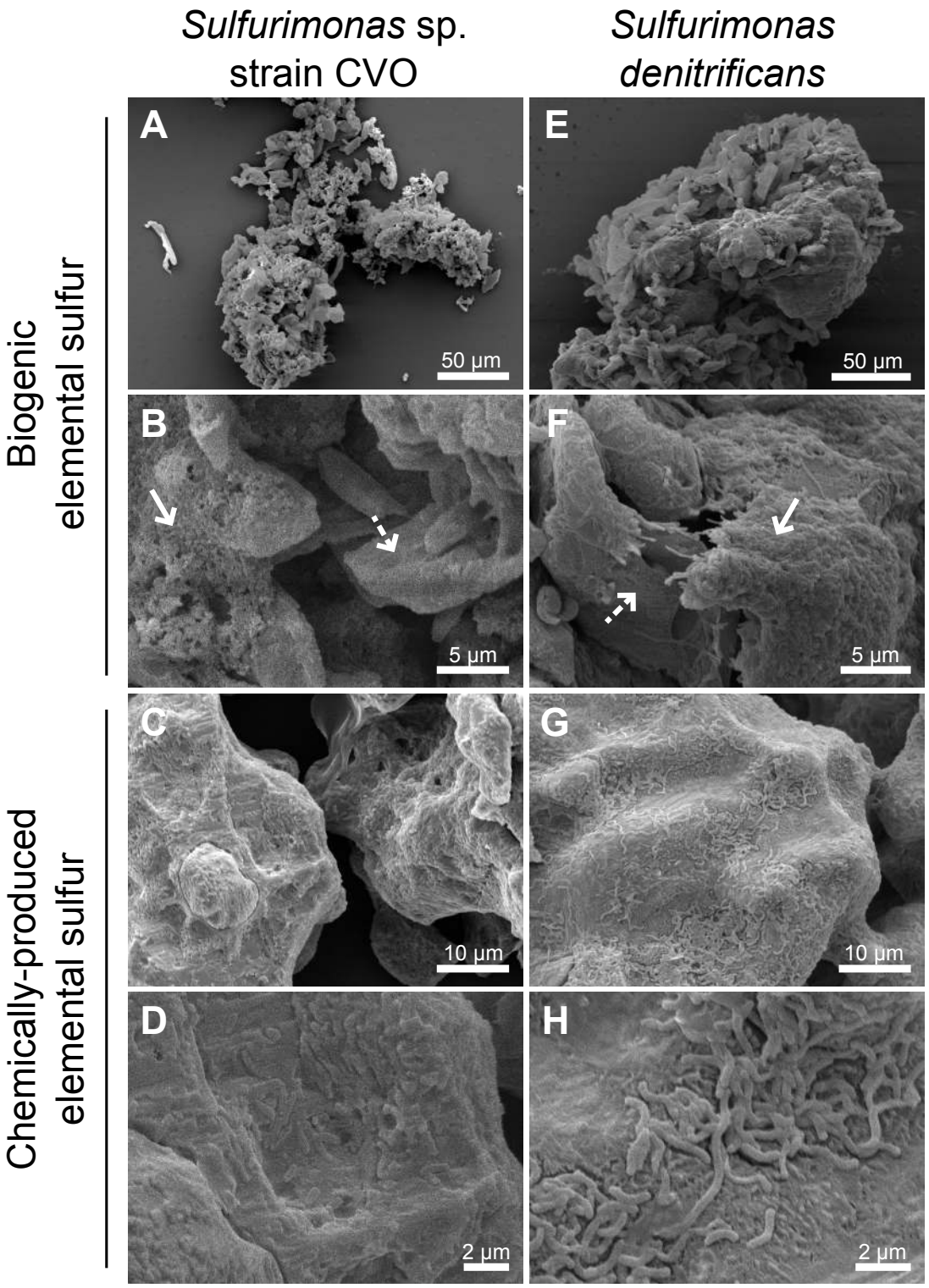

Figure S7 Scanning electron micrographs of zero-valent elemental sulfur particles retrieved from cultures of *Sulfurimonas* sp. strain CVO (A-D), *Sulfurimonas denitrificans* DSM 1251 (E-H). The arrows indicate biofilm covered (solid line) or free surfaces (dashed line).

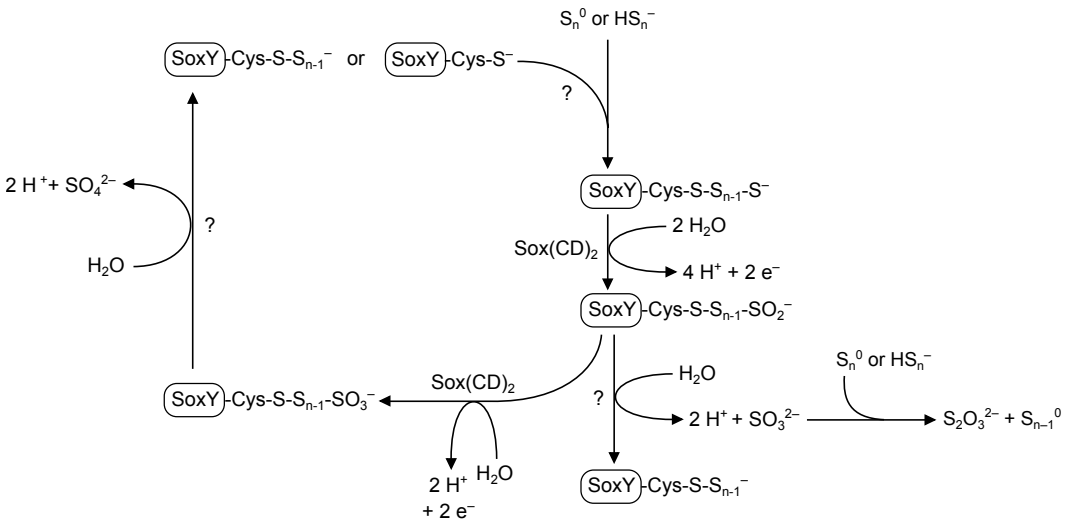

Figure S8 Proposed model for the oxidation of SoxY-bound sulfur and formation of sulfite in *Sulfurimonas* sp. strain CVO. Sulfite is proposed to then abiotically react with either zero-valent elemental sulfur or polysulfides to form thiosulfate. The activation mechanism of zero-valent sulfur and the hydrolysis steps that release sulfate or sulfite are currently unknown and marked with a question mark (?).